6th Ablation Workshop

April 10-11th 2014
I Hotel and Illinois Conference Center
1900 S. First Street, Champaign, IL 61820
http://ablation2014.engineering.uky.edu

Hosted and organized by

UK University of Kentucky

Illinois University of Illinois at Urbana-Champaign

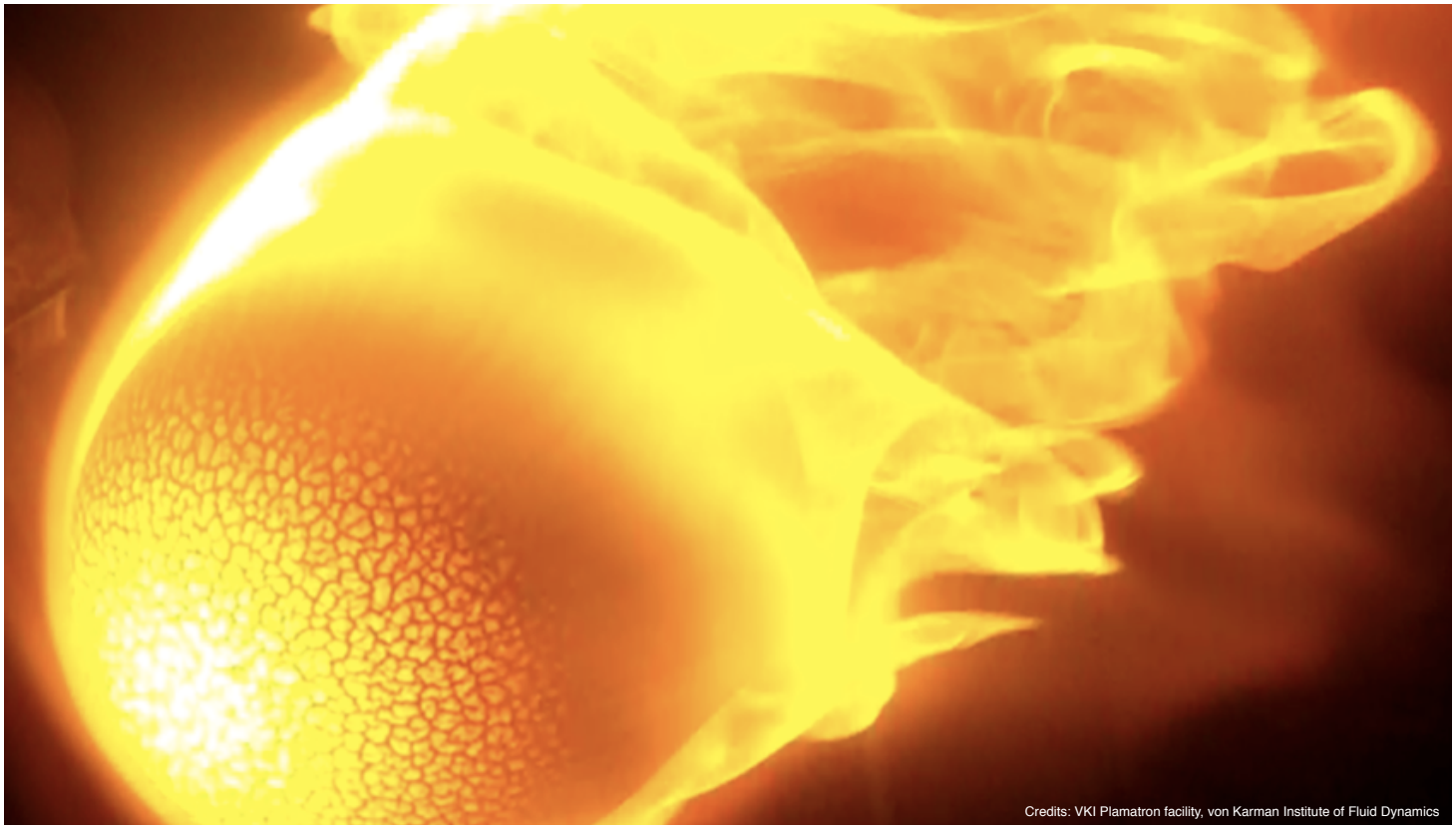

Credits: VKI Plamatron facility, von Karman Institute of Fluid Dynamics

Steering Organizations

Sandia National Laboratories

NASA

AFOSR Air Force Office of Scientific Research

Proceedings of the 6th Ablation Workshop

Sponsored by

NASA Kentucky Space Grant Consortium and EPSCoR Programs

NASA

Proceedings of the 6th Ablation Workshop
Urbana-Champaign, IL,

Edited by
Alexandre Martin
University of Kentucky

April 10 – April 11, 2014

Published by:
6th Ablation Workshop,
http://ablation2014.engineering.uky.edu

Credits:
Cover design: Alexandre Martin
Cover image: *Ablative material in the Plasmatron facility*, von Karman Institute of Fluid Dynamics
LaTeX editor: Alexandre Martin, Huaibao Zhang and Haoyue Weng (using LaTeX's 'confproc' package, version 0.8 by V. Verfaille)

Printed in Lexington, Kentucky, April 1, 2014.

CONFERENCE PROGRAM

Day 1: April 10, 2014

Introduction and Overview

New Developments in Ablation Science - Modeling

Ablation Test-cases

Day 2: April 11, 2014

New Developments in Ablation Science - Materials

New Developments in Ablation Science - Experiments

ABLAMOD: ADVANCED ABLATION CHARACTERIZATION AND MODELING EUROPEAN PROJECT DESCRIPTION

G. Pinaud
Airbus Defence and Space
Saint-Médard en Jalles, France
gregory.pinaud@astrium.eads.net

A. Guelhan
German Aerospace Center (DLR)
Cologne, Germany
ali.guelhan@dlr.de

In order to sustain Europe activities whether it would be in deep space, across the solar system or on low Earth-orbit for a long term, it is essential that technologies with key capabilities are at Europe disposal. This status requires developments of radical innovation which may then lead to disruptive applicative technologies. Within this context, new thermal protection system and reliable strategies for sample return missions are defined as European priorities in a short future. In Europe, the design of spacecraft for high-energetic interplanetary or sample return atmospheric flights are still performed with huge safety margins at every link of the sizing chain. Consequently, spacecraft mass budgets are far to be optimized and therefore limiting the scientific interests.

In order to improve the design tools for Spacecraft, the Europe funded ABLAMOD project started in January 2013 and involved a consortium of 10 company and institutes: DLR (G, Coordinator), ACC (P), Airbus Defence and Space (F), Avio (I),CIRA (I), FGE (UK), Uni. of Starthclyde (UK), VKI (B), AIT (AUT), OGI (AUT). The ABLAMOD project aims indirectly at reducing modeling uncertainties by improving the flow characterization of arc heated facilities (DLR L2K/L3K, CIRA SIROCCO) used for ablator testing and by applying new methods for the prediction of ablation and degradation processes of 3 different ablators. These thermal protection materials are a light weight carbon phenolic resin (ASTERM manufactured by Airbus Defence and Space), a cork based material (TPS3L manufactured by Amorim Cork Composite) and a silicon based material (SV2, manufactured by Avio).

To fulfill the technical objectives, the project is divided in the following elementary characterization, plasma flow diagnostic technics and theoretical modeling work-package:

- WP2: Definition of system requirements including material sample manufacturing, characterization, instrumentation
- WP3: Recession measurement technique, upgrading the broadband CARS technique (Coherent Anti-Stokes Raman Scattering), implement O-LIF (Laser Induced Fluorescence), DLAS (Diode Laser Absorption Spectroscopy) and Emission Spectroscopy technique in ground testing facilities
- WP4: Test plan in L2K/L3K, SCIROCCO arc heated facilities, characterization of the high enthalpy flow conditions, determination of material response at moderate and high enthalpies plasma
- WP5: Flow simulation, material response pre-test modelling, implementation of module for transport properties and radiation, for material internal flow simulation, for gas surface interaction and finally a post-test modelling and extrapolation to flight

As a results, the experimental characterizations of the material families together with the most advanced diagnostic plasma flow techniques will bring numerous and valuable data which would enable the elaboration of the finest and reliable ablation and degradation model.

The exploitation of these disruptive approaches and model will help the industrial partner in their design, sizing optimal and robust spacecraft.

ABLATOR RESPONSE MODEL DEVELOPMENT AND CHALLENGES

Nagi N. Mansour
NASA Ames Research Center
Moffett Field, California
nagi.n.mansour@nasa.gov

Jean Lachaud
University of California, Santa Cruz
Moffett Field, California
jlachaud@ucsc.edu

Thierry Magin
von Karman Institute for Fluid Dynamics
Brussels, Belgium
alessandro.turchi@uniroma1.it

The successful Mars atmospheric entry by the Mars Science Laboratory [1] (MSL-Curiosity) combined with the success of the Earth atmospheric entry by the Stardust capsule [2] have established PICA [3] as a major Thermal Protection Systems (TPS) material. We expect that this class of materials will be on the short list selected by NASA for any atmospheric entry missions and that it will be the lead of that list of materials in any planning, feasibility studies or flight readiness studies. In addition to NASAs successes, the Dragon capsule [4], the successful commercial space vehicle built by SpaceX, uses PICA-X, while the European Space Agency is considering ASTERM [5]for its exploration missions that involve atmospheric entries, both of these materials are of the same family as PICA.

The motivation for the current effort is to enable optimized risk and margin recommendations by building models that are based on a fundamental understanding of the material behavior and validating the models with ArcJet/Plasmatron and flight data.

Current material response models are inspired by the model of Kendall et al. published in 1968. They are based on five major assumptions: 1) pyrolysis gases are in equilibrium in the material; 2) pyrolysis gases are transported by convection only; 3) air does not penetrate inside the material; 4) ablation only occurs at the surface; 5) the solid at the surface is in chemical equilibrium with the gas. Since 1968 a few attempts have been made to introduce finite-rate chemistry models both for the pyrolysis gases and at the surface. Unfortunately, these models are mostly heuristic and not trusted for design. In other words, of all the extremely complex phenomena occurring in a porous ablative material, only Fouriers heat transfer and the pyrolysis of the solid are rigorously modeled. Interestingly, this approximate model has been able to reproduce, within a reasonable accuracy, Arc Jet performance tests carried out on PICA in conditions relevant to NASAs missions. Therefore, depending on the design layout and quantity of interest, current models are robust. In off-design conditions, however, there is a strong need to improve current models.

In the talk, a high-fidelity model (type 3, see figure) will be detailed and discussed. The model tracks the chemical composition of the gases produced during pyrolysis. As in the conventional models, it uses equilibrium chemistry to determine the recession rate at high temperatures but switches to in-volume finite-rate ablation for lower temperatures. It also tracks the time evolution of the porosity of the material. Progress in implementing this high-fidelity model in a code will be presented. In addition, a set of basic experimental data being supported for model validation will be summarized. The validation process for the model development will be discussed. Preliminary results will be presented for a case where detailed pyrolysis product chemistry is computed. Finally, a wish list for a set of validation experiments will be outlined and discussed.

1. REFERENCES

[1] http://www.jpl.nasa.gov/spaceimages/details.php?id=PIA12117

[2] http://stardust.jpl.nasa.gov/home/index.html

[3] Tran, H. K., Johnson, C. E., Rasky, D. J., Hui, F. C. L., Hsu, M.-T., Chen, T., Chen, Y. K., Paragas, D., and Kobayashi, L. NASA, TM 110440, 1997.

[4] http://www.spacex.com/dragon.php

[5] H. Ritter, O. Bayle, Y. Mignot, P. Portela, J-M. Bouilly, R. Sharda, 8th International Planetary Probe Workshop (IPPW-8) Portsmouth 6-10 June 2011.

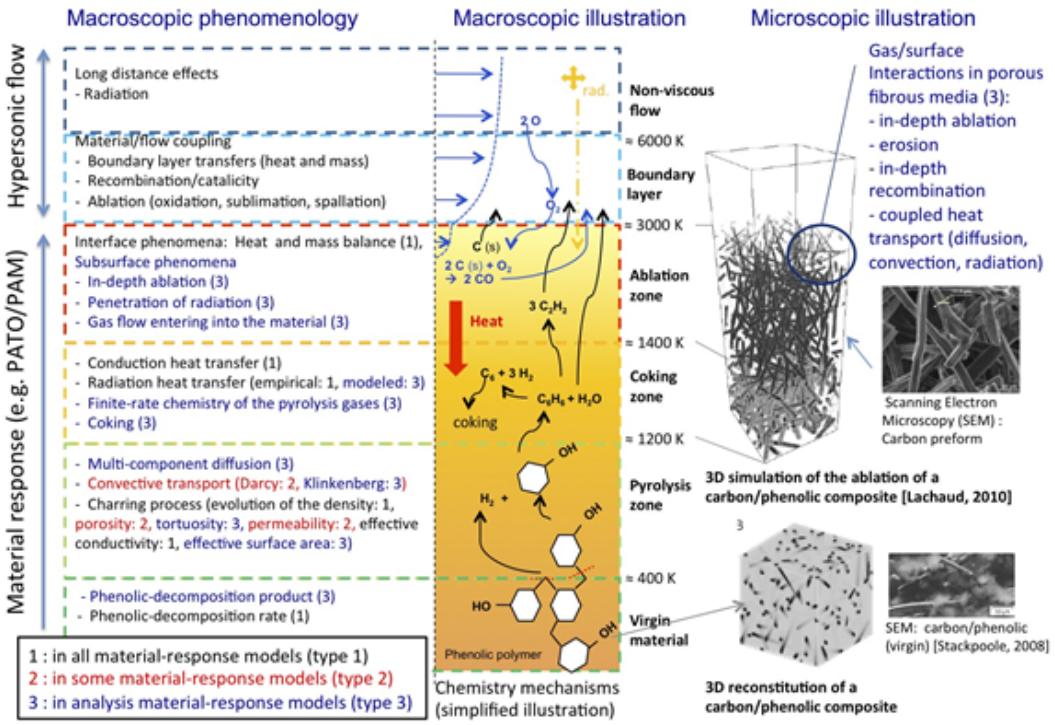

NUMERICAL AND EXPERIMENTAL INVESTIGATIONS OF ABLATIVE THERMAL PROTECTION SYSTEM SURFACE DEGRADATION EFFECTS ON NEAR-WALL FLOW

Alexandre Martin

Department of Mechanical Engineering
University of Kentucky
Lexington, KY

Sean Bailey

Department of Mechanical Engineering
University of Kentucky
Lexington, KY

Although immensely successful, recent data from the Mars Science Lab entry confirms the need to better understand and model the complex aero-thermal environment of TPS material interaction with the flow field. The present study aims at understanding the complex phenomenon necessary to develop the high fidelity tools needed for a detailed characterization of the near wall flow and chemical composition. With these tools, our ability to model and predict deterioration of TPS and associated effects on the surrounding flow field will be improved.

Specifically, the boundary layer interactions, as well as their influence on near wall flow is investigated [Ref.1]. These effects include surface roughness and pyrolysis gas injection effects on boundary layer turbulence structure and transport. The transport of the pyrolysis gas inside the ablator is also studied, and the geometrical effects are quantified [Ref. 3]. Finally, spalled particles ejected from the ablated surface are modeled, and their effect on the flow field are discussed [Ref. 2].

1. REFERENCES

[1] Miller, M. A., Martin, A., and Bailey, S. C. C., "Investigation of the scaling of roughness and blowing effects on turbulent channel flow." *Experiments in Fluids*, Vol. 55, No. 1675, 2014.

[2] Davuluri, R. and Martin, A., "Numerical study of spallation phenomenon in an arc-jet environment," *11th AIAA/ASME Joint Thermophysics and Heat Transfer Conference*, AIAA Paper 2014-xxxx, Atlanta, GA, 16 - 20 June 2014, Accepted (Manuscript 1890802).

[3] Weng, H. and Martin, A., "Numerical study of geometrical effects on charring ablative arc-jet samples," *International Journal of Heat and Mass Transfer*, 2014, Submitted (Manuscript HMT-S-14-00638).

INVESTIGATION OF SURFACE RADIATION IN EARTH RE-ENTRY FLOWS WITH GRAPHITE ABLATION

C. R. Alba and R. B. Greendyke

Department of Aeronautics and Astronautics
AFIT, Wright-Patterson AFB, OH
christopher.alba@afit.edu

S. Lewis, G. C. Looringhe, T. Eichmann and R. Morgan

Centre for Hypersonics
University of Queensland, St Lucia, Australia
r.morgan@uq.edu.au

Thermal protection systems (TPS) are subjected to severe thermal and mechanical loads when exposed to hypersonic re-entry environments and must be designed to prevent excessive heat from damaging the vehicle. The materials used for TPS interact with the flow through various thermochemical and thermophysical processes such as ablation, spallation, thermal conduction, and radiative transport. Surface chemical reactions play a prominent role in determining ablation and energy transfer rates. Hence, the correct understanding and accurate modeling of the gas-surface interaction phenomena plays an integral part in the design of TPS for re-entry vehicles. To examine these phenomena in more detail, a series of high speed flow experiments were conducted in the X2 facility at the University of Queensland, Australia. The X2 facility is a shock expansion tunnel that can be used to test subscale models at realistic flight temperatures and enthalpies [1, 2]. The model used in the experiments was a short half-cylinder made of isomolded graphite tested at an 8.5 km/s Earth entry velocity monitored by ultraviolet (UV) spectrometry. The experiments utilized a new concept of pre-heating the model to temperatures in excess of 2000 K to stimulate surface reactions and increase ablation during the microseconds of available test time [3]. The nonequilibrium chemistry occurring in the shock layer was investigated by making calibrated measurements of the spectral radiance emitted by the CN molecule. Hypersonic nonequilibrium, ablating simulations were performed to support these experiments using high-fidelity computational fluid dynamic (CFD) and radiation codes. Two air-carbon gas-surface chemistry models attributable to Park [4, 5] and Zhluktov and Abe [6] were implemented into the CFD code as a boundary condition.

The presentation will provide preliminary results of how the simulated spectral radiance compared to the experimental measurements. The validity of the physical models used in the simulations will also be discussed. Both surface reaction models overpredicted the radiative heat flux compared to the experiment. However, the radiative heating predictions provided by the Zhluktov and Abe model were more sensitive to wall temperature and reflected experimental ablation rate trends. Further, there were notable differences in the predicted surface mass fluxes and mass fractions for other species than CN that highlight the differences in the surface modeling approaches. The best comparison was found when modeling the wall as isothermal and not including surface reactions. These results are very interesting that suggest varying conclusions and lead to more questions for future investigations.

1. REFERENCES

[1] Morgan, R. G., McIntyre, T. J., Buttsworth, D. R., Jacobs, P. A., Potter, D. F., Brandis, A. M., Gollan, R. J., Jacobs, C. M., Capra, B. R., McGilvray, M., and Eichmann, T., "Impulse facilities for the simulation of hypersonic radiating flows," AIAA Paper 2008-4270, 2008.

[2] McIntyre, T. J., Eichmann, T. N., Jacobs, C., Potter, D., McGilvray, M., Jacobs, P., and Morgan, R., "Shock Tube and Expansion Tunnel Measurements of High Temperature Radiating Flows," *Proceedings of the 4th International Workshop of Radiation of High Temperature Gases in Atmospheric Entry*, Lausanne, Switzerland, October 2010.

[3] Zander, F., Morgan, R. G., Sheikh, U., Buttsworth, D. R., and Teakle, P. R., "Hot-Wall Reentry Testing in Hypersonic Impluse Facilities," *AIAA Journal* , Vol. 51, No. 2, February 2013, pp. 476-484.

[4] Chen, Y. and Milos, F. S., "Finite-Rate Ablation Boundary Conditions for a Carbon-Phenolic Heat-Shield," AIAA Paper 2004-2270, 2004.

[5] MacLean, M., Marschall, J., and Driver, D. M., "Finite-Rate Surface Chemistry Model, II: Coupling to Viscous Navier-Stokes Code," AIAA Paper 2011-3784, 2011.

[6] Zhluktov, S. V. and Abe, T., "Viscous Shock-Layer Simulation of Airflow past Ablating Blunt Body with Carbon Surface," *Journal of Thermophysics and Heat Transfer*, Vol. 13, No. 1, January-March 1999.

UNCERTAINTY ANALYSIS OF CARBON ABLATION IN THE VKI PLASMATRON

Alessandro Turchi
Aeronautics and Aerospace Department
von Karman Institute for Fluid Dynamics
alessandro.turchi@vki.ac.be

Pietro M. Congedo
INRIA Bordeaux Sud-Ouest

Bernd Helbe
Aeronautics and Aerospace Department
von Karman Institute for Fluid Dynamics

Thierry E. Magin
Aeronautics and Aerospace Department
von Karman Institute for Fluid Dynamics

Inductively coupled plasma (ICP) torch facilities are commonly used to simulate atmospheric re-entry conditions and to test possible thermal protection system material candidates. Several simulation campaigns took place at the VKI over the past years to advance the fundamental knowledge of ablation phenomena. Ablation tests of several materials, from pure graphite to newer low-density pyrolyzing materials, have been carried out in air/nitrogen plasmas in the Plasmatron. The fully instrumented Plasmatron test chamber allows the accurate monitoring of the freestream conditions during the tests, as well as the measurements of some material responses as the recession rate and the surface temperature. Modeling and simulation of the gas surface interaction (GSI) over ablative surface could be used aside the experimental tests to improve the physical understanding and to support the development of new generation thermal protection system (TPS) materials. In this frame, the goal of the present contribution is to investigate the influence of experimental and model uncertainties on the final quantities of interest (QOIs) for the ablative material response characterization (i.e. mass blowing rate, surface temperature, wall heat flux).

To fully characterize these experimental tests, the boundary layer edge conditions have to be rebuilt. This rebuilding is performed by means of a standard procedure based on the Local Heat Transfer Simulation (LHTS) concept[1] and involves both numerical simulations and experimental measurements. In order to do so, a stagnation point heat flux probe and a Pitot probe, having the same geometry as the TPS sample, are used for the characterization of the plasma flow at the location of the test sample during the Plasmatron test. These measurements provide a cold-wall reference heat flux ($\dot{q}_{cw}$, $T_{cw} \sim 350$K) and a dynamic pressure measurement (p_d), and are integrated with the record of the test chamber static pressure (p_s). Then, in the first step of the rebuilding procedure, the ICP subsonic flow is simulated, under the hypothesis of local thermochemical equilibrium, by means of the *VKI ICP code* imposing the test mass flow rate, the torch power and the measured chamber static pressure. Subsequently, the outputs of this simulation and the experimental measurements, are used together in the *VKI Boundary-layer* code to rebuild the boundarylayer edge conditions.

This rebuilding procedure involves multiple boundary-layer simulations that use the non-dimensional parameters characterizing the dynamic boundary layer and iterate on the outer edge temperature until the measured cold-wall heat flux is matched. Unfortunately these simulations are prone to a series of epistemic and aleatory uncertainties on both input values and modeling parameters. An uncertainty quantification analysis has already been performed to study the impact of these uncertainties on the rebuilt catalycity of reusable TPS materials[2]. Experimental measurements were considered as aleatory variables having a normal probability density function (PDF). The effective catalytic re- combination coefficient of the copper calorimeter (γ_{ref}) was considered as an epistemic uncertainty, and its influence on the rebuilt edge conditions was also analyzed. In the present work a similar analysis will be repeated considering the Plasmatron operative condition of the selected ablative sample test. Moreover, considering the importance of the mixture composition on the accurate evaluation of the ablation QOIs, the impact of slightly modified boundary-layer edge elemental compositions (x_N/x_O), caused by the possible elemental diffusion through the Plasmatron chamber (not considered in the ICP chamber simulation), will be also investigated. When dealing with ablative test samples, the rebuilt edge conditions are then used as free-stream boundary conditions for the *VKI Stagnationline code* that integrates a GSI routine to solve for the surface ablation of the TPS material. The ablation modeling is based on the surface mass and energy balances over ablative materials that can be derived directly from the observation of the involved phenomena. In the case of non-pyrolyzing ablative materials, the considered surface balances read:

$$\rho D_{im} \frac{\partial y_i}{\partial r}\bigg|_w + \dot{m}_c y_{i_c} = (\rho v)_w y_{i_w} \quad i = 1, N_s \tag{1}$$

which is the surface mass balance (SMB) for the i^{th} species, and:

$$k \frac{\partial T}{\partial r}\bigg|_w + \sum_i^{N_c} h_{i_w} \rho D_{im} \frac{\partial y_i}{\partial r}\bigg|_w + \dot{m}_c h_c = (\rho v)_w h_w + \sigma \varepsilon_s T_w^4 + \dot{q}_{ss} \tag{2}$$

hich is the surface energy balance (SEB). Since no coupling with a material solver is considered, the steady-state ablation hypothesis is used to evaluate the solid conduction term ($\dot{q}_{ss}$) and close the SEB. Because of the lack of a proper gas-radiation model, the gas radiation is neglected in Eq. 2, and only the surface re-radiation is accounted for. The SMB and the SEB combined with a suitable ablation model, provide complete surface thermochemistry conditions for the numerical solution of the coupled CFD/ablation problem for TPS analysis. In the present work, the considered finite-rate gas-surface interaction model for the carbon-based material consists of two oxidation, a nitridation and a sublimation surface reactions[3]. Further analyses arose the needing of considering an additional phenomenon that could take place at the material surface: the $N \rightarrow N_2$ recombination. This highly exothermic process was considered as an additional surface reaction whose reaction probability was taken from the literature[4]. At this point, it is worthwhile noting that, although this finite-rate ablation model potentially represents a more accurate representation of the GSI than other rather simplified boundary conditions (i.e. radiative equilibrium with imposed blowing, equilibrium ablation, etc...), its basis on several modeling parameters as the heterogeneous reaction probabilities is an issue. A critical review of these quantities would require dedicated and complicated numerical/experimental joint works, sometimes practically infeasible due to the measurement difficulties/impossibilities in the harsh conditions of interest for re-entry applications. For this reason, the reaction probabilities of the surface heterogeneous and homogeneous reactions will be considered as epistemic variables in the present work and their influences on the final quantity of interests will be assessed in the analysis.

A stochastic polynomial-chaos method will be used in this work to deal with the uncertainty propagation. This method will be applied serially, first to the boundary-layer edge condition rebuilding and then to the evaluation of the final QOIs (steady-state surface temperature, mass blowing rate of the TPS and hot-wall heat flux). Two different surrogate models of the *VKI Boundary-layer code* and of the *VKI Stagnation-line code* will be created. Using this non-intrusive uncertainty quantification approach, a single deterministic computation is replaced with a whole set of stochastic computations, each one of those being run for specific values of the uncertain input conditions. Figure 1 shows a typical output of this analysis. The considered material is a carbon-preform. This compound consists of randomly oriented carbon fibers with a density typically ranging between 180-210 kg/m^3 and a porosity of 90%. The ablative test sample is a hemispherical probe with 2.5 cm nose radius. The influences of the ablation model parameters on the computed mass blowing rate and surface temperature are shown. It is interesting to note that, in the particular considered case, the oxidizing reaction probability uncertainties have a negligible influence on the QOIs (although the majority of the mass blowing rate can be attributed to the surface oxidation by the atomic oxygen). This can be attributed to the particular ablation regime that is established for the oxidation reactions: the diffusion-limited regime. Differently, both surface nitridation and surface nitrogen recombination play a major role in the final QOI uncertainties. The latter, in particular, has the strongest effect on the determination of the wall temperature and indirectly influences the surface ablation through the modification of the nitrogen concentration next to the surface. This preliminary results shows the importance of a thorough uncertainty analysis that should help in defining those critical modeling parameters or experimental measurements that have to be carefully reviewed or updated in order to reduce the uncertainties on the prediction of the selected QOIs. This objective will be pursued in the final work.

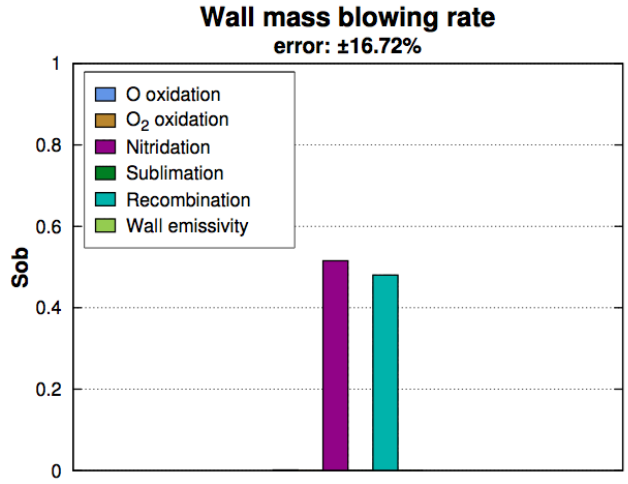

(a) Mass blowing rate

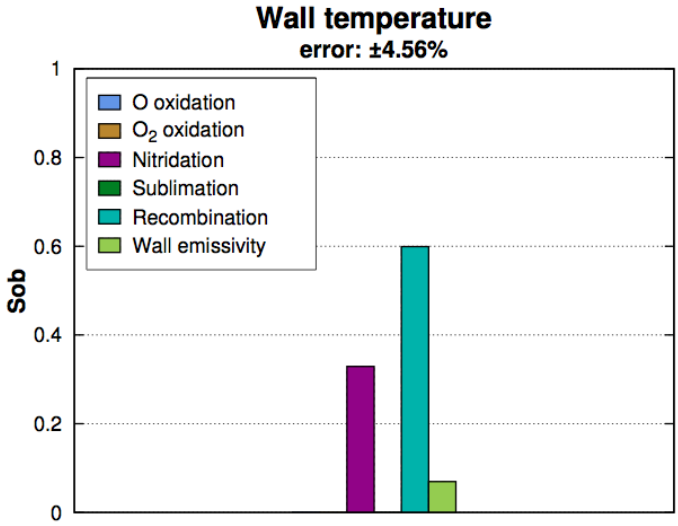

(b) Surface temperature

Figure 1: Example of uncertainty analysis output: Sobol influence indexes.

1. REFERENCES

[1] Barbante, P. and Chazot, O., "Flight Extrapolation of Plasma Wind Tunnel Stagnation Region Flowfield," *Journal of Thermophysics and Heat Transfer*, Vol. 20, No. 3, 2006, pp. 493-499.

[2] Villedieu, N., Panerai, F., Chazot, O., and Magin, T., "Uncertanity Quantification for Gas-Surface Interaction in Plasmatron Facility," *Proceedings of 7th European Symposium on Aerothermodynamics for Space Vehicles*, May 2011, ESTEC, ESA SP-692, Noordwijk, The Netherlands, 2011.

[3] Park, C., Jaffe, R. L., and Partridge, H., "Chemical-Kinetic Parameters of Hyperbolic Earth Entry", *Journal of Thermophysics and Heat Transfer*, Vol. 15, No. 1, 2001, pp. 7689.

[4] Driver, D., Olson, M., Barnhardt, M., and MacLean, M., "Understanding High Recession Rates of Carbon Ablators Seen in Shear Tests in an Arc Jet," AIAA Paper 20101, 2010, 48th AIAA Aerospace Sciences Meeting including the New Horizons Forum and Aerospace Exposition, Orlando, Florida, January 4-7, 2010.

MATERIAL RESPONSE CHARACTERIZATION OF NEW-CLASS ABLATORS IN VIEW OF NUMERICAL MODEL CALIBRATION AND VALIDATION

Bernd Helber

von Karman Institute for Fluid Dynamics
& Vrije Universiteit Brussels, Brussels, Belgium
helber@vki.ac.be

Alessandro Turchi and Thierry Magin

von Karman Institute for Fluid Dynamics
Brussels, Belgium
alessandro.turchi@uniroma1.it

A critical problem for safety of astronauts and embarked payload is the thermal protection system and the associated material response model, required for prediction of the material performance and determination of the heat shield thickness. New multi-scale material response models are proposed in order to take into account the porous micro-structure of the new class of materials but experimental data are needed for the understanding of the material response under extreme heating conditions and validation of new numerical tools. Our research aims at understanding important phenomena in gas-surface- and materials science, for example, the influence of the test environment on the surface recession, the pyrolysis gas chemistry within the material, and transport phenomena in the reactive boundary layer. With this work we started a closer study of the ablative behavior of a non-pyrolizing carbon fiber preform and the carbon-phenolic ablator AQ61.

All ablation experiments of various materials were carried out in the 1.2 MW Plasmatron facility at the von Karman Institute, which is extensively utilized for the simulation of reentry plasma flows. It is a state-of-the-art facility and presently the most powerful inductively coupled plasma (ICP) torch in the world. It was developed during the 90's to fulfill the need of specific tools for the development and testing of new TPS within Europe. As the gas is heated by induction through a coil, one of the advantages of ICP torches, with respect to Arc-jet facilities, is the high purity of the plasma flow thanks to the absence of electrodes and their associated erosion. This particular characteristic makes the ICP plasma generators a perfect facility for the study of the complex gas-surface interaction, such as ablation and catalysis, where the chemical interaction between the gaseous species, and the solid material constituents is the driving phenomenon and a precise control of the flow conditions is sought. For these reasons, several simulation campaigns took place at the VKI over the past years to advance the fundamental knowledge of ablation phenomena. Ablation experiments of various materials, from pure graphite to newer low-density pyrolyzing materials, have been carried out in air and nitrogen plasmas. The facility offers calibration of the plasma free-stream in terms of pressure and heat flux measurements prior to the ablation test, which deliver input to an extensive numerical rebuilding procedure that offers a detailed characterization of the boundary layer, and extrapolation of ground-test data to real flight conditions. A comprehensive experimental setup, designed for ablation studies, enables online quantification of the recession rate, surface temperature, and spatially resolved boundary layer radiation by emission spectroscopy. These features make the data collected from the ablation experiments rather unique, generating a wide data set for ablative model calibration and validation.

Several numerical tools were recently developed at the VKI in order to be used for the investigation of reentryrelated phenomena. A new thorough library (Mutation++) for the evaluation of thermal and transport properties of gas mixtures has been developed. This has further been extended to calculation of both finite-rate gas-phase chemistry and homogeneous/heterogeneous gas/gas-solid equilibrium chemistry. The Mutation++ library has been coupled with a stagnation-line code including an ablating boundary condition, able to reproduce the stagnation line properties of a spherical or cylindrical ablating body. The ablation model is based on a general control volume approach, solving mass balance, and energy balance equations at the surface.

Spatially resolved emission spectroscopy enabled reconstruction of the CN violet system emission profile within the boundary layer. The results of the stagnation line description with ablative boundary condition, together with the Specair radiation tool, were used to produce numerically estimated emission profiles for a preliminary comparison. Although a reduced numerical model was used in combination with a very simplified approach to compute the spatial boundary layer emission, intensities were in the same order of magnitude compared to the experimental data for various test conditions. The model was further able to predict the location of the maximum emission in a high pressure environment, changing from 2.5 mm-1.5 mm from the wall when the heat flux was tripled. Most measured mass blowing rates were in a diffusion limited ablation regime, although several cases at high surface temperature exist which led to high mass loss. For low pressures of 15 hPa, the numerical model almost matched the experimentally determined mass blowing rate, and surface temperatures are

as close as 200 K. Based on experimental results in nitrogen plasmas, the recombination efficiency to molecular nitrogen at the ablating surface will be objective of future investigations.

MICROSCALE MODELING OF ABLATIVE THERMAL PROTECTION SYSTEM MATERIALS

Eric Stern
University of Minnesota
stern177@aem.umn.edu

Graham Candler
University of Minnesota
candler@aem.umn.edu

Tom Schwartzentruber
University of Minnesota
schwartz@aem.umn.edu

ABSTRACT

Modeling the performance and behavior of thermal protec- tion system (TPS) materials as they undergo the extreme conditions of atmospheric entry is a very complicated and challenging problem. Historically, models have generally been of the volume-averaged variety, and the various closures found within them have involved a great deal of empiricism. Recently, some researchers have taken the the approach of modeling the materials at the microscale (Lachaud et. al) in order to gain insight into the complex phenomena, as well as inform volume-averaged models. In this presentation we will give an overview of efforts underway at the University of Minnesota to develop a high fidelity microscale material response modeling capability. Here, we provide a brief overview of the activities which we will discuss in greater detail at the workshop.

Methodology

One of the challenges of attempting to model this type of flow at this scale is the fact that, because the fibers that make up the TPS material are very small ($\approx$ 1 to 10 μm), the mean free path of the molecules and atoms in the gas is often on the order of the fibers themselves. When this is the case, the Navier-Stokes equations, which are based on a continuum assumption, are no longer valid. For the majority of analysis we will present, we have chosen to employ the Direct Simulation Monte Carlo (DSMC) method to model the gas phase, and gas-surface interaction phenomena. DSMC is a stochastic particle based method, which is valid (given that you have the computational resources) for all Knudsen numbers - Knudsen number being the ratio between the mean-free-path of the gas and a relevant length scale of the problem - in our case the fiber diameter, or the pore diameter. The Molecular Gas Dynamics Simulator (MGDS) code has been developed at the University of Minnesota. It is a parallel implementation of the DSMC method, with many features that make it attractive for doing this type of problem, including its ability to handle complicated geometries using a robust cut-cell algorithm. Additionally, the DSMC method inherently handles non-equilibrium phenomena, as well as potentially provides a framework for more physics-based gas-surface interaction models. Figure 1 shows an example of steady flow calculations of a porous structure similar to those found in TPS materials. It is shown here to demonstrate the use of the cut-cell to embed complicated surfaces in a cartesian mesh. In the presentation we will provide further detail on some of the modifications made to the code to enable these types of simulations.

Surface Generation

As we are proposing to improve the fidelity of material response modeling by simulating the microstructure of the TPS materials, me must have a framework for generating computational surface meshes which approximate said microstructures. To this end, we have developed a method for generating random arrays of non-overlapping fibers, where we can control the distributions of three-dimensional orientations, fiber diameters, bulk porosity, etc. We will use this capability to demonstrate

the effects of some microstructural parameters on performance, as well as present evolution of some fiber characteristics (i.e diameter, and bulk density) over time for coupled simulations. Figure 2 shows an example of a surface generated using this code. In this example, we have allowed the fibers to vary about a nominal radius, and orientation. In addition, we have specified a density profile in the material to emulate a porous material which has undergone in-depth ablation. This code has been developed in such a way that it can be coupled to the DSMC flow solver, so that we can update the surface on-the-fly to simulate the ablation of the fibers.

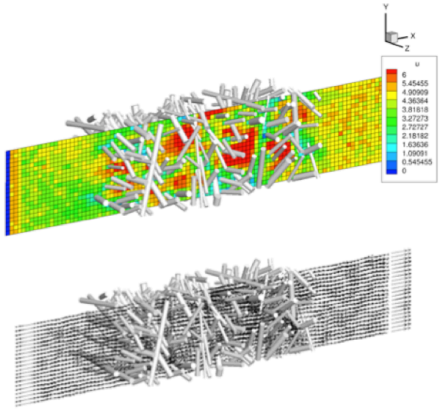

Figure 1: Visualizations showing contours of x-velocity (top), and velocity vectors (bottom) for flow through a porous medium.

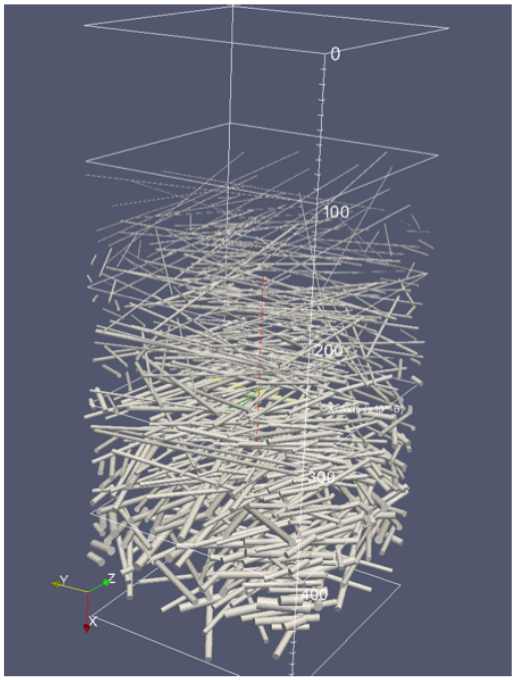

Figure 2: Example of a FiberForm-like surface which has undergone a prescribed volume ablation.

Application to Permeability

One immediate application of this capability is the computation of permeability coefficients for porous media convection models, such as Darcys Law. Most volume averaged ablation models in use today use a variation of Darcys law to model the flow of gas through porous TPS materials. By simulating the flow through the microstructure and measuring the mass flux and pressure, we can compute the coefficients used in these models directly. In addition, we use both CFD computations and empirical models of these coefficients to provide verification and validation of our methodology. Figure 3 shows the computed permeability for regular arrays of cylinders for both DSMC and CFD (with a slip wall model) versus the porosity of each configuration. These are also compared to an empirical model from the literature. In the near-continuum limit, we observe very good agreement between the two methods, as well as good agreement with the model. However, when the Knudsen is sufficiently large, we observe deviation between the methods, and the models. In this case of transitional flow, the assumptions underlying the CFD and the model are no longer valid, and a method such as DSMC must be used to properly capture the physics.

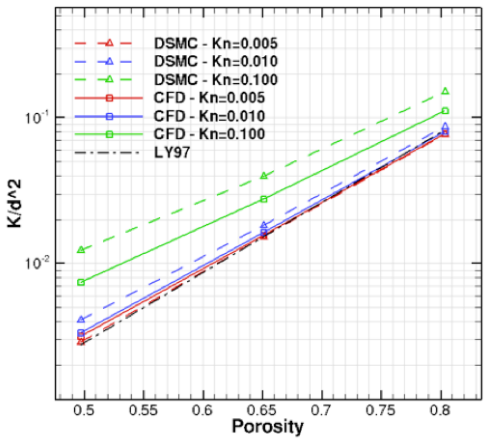

Figure 3: Permeability results for a regular array of cylinders in a “square” configuration.

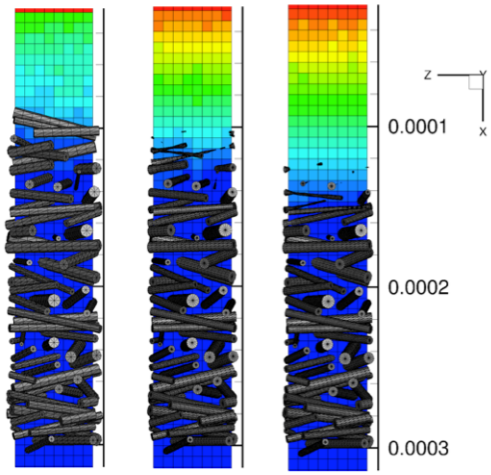

Figure 4: Visualizations at various times for a coupled simulation where fibers ablate based on surface reactions.

Coupled Ablation

Ultimately, the goal of this approach will be to simulate fully coupled material response at the microscale. Work in this area is very much on-going on several fronts - surface chemistry models, proper boundary conditions, gas-phase chemistry modeling, surface reconstruction methods, etc.. Figure 4 shows a demonstration of the progress made toward developing such a capability. Here we show results from a simple case devised to demonstrate the coupling. In this case we allow O2 to diffuse in from the top of the domain. The gas-surface interaction is modeled with a single reaction ($O_2 + C_s \rightarrow CO_2$). In DSMC, surface reactions are modeld by determining a probability that, when a particle strikes a surface, it will react. For the purposes of this demonstration, we have set this probability to unity, however developing and implementing better models is an area of on-going research. In fact, this is another reason that the DSMC method is at- tractive, as it provides a more straight forward framework for application more high fidelity chemistry models, as these are often based on a molecular perspective. For the presentation, we will present some results for more complicated systems, with varying reaction parameters, as well as discuss potential modeling strategies going forward.

ACKNOWLEDGMENTS

The primary author is supported by a NASA Space Technology Research Fellowship through the NASA Office of the Chief Technologist under training grant # NNX11AN42H.

DEVELOPMENT OF MODELING CAPABILITIES FOR DECOMPOSING ABLATORS

Roy Hogan, David Kuntz, Micah Howard, and Ben Blackwell

Sandia National Laboratories

rehogan@sandia.gov

Sandia National Laboratories has a history of supporting DOE missions by analyzing, designing, and building thermal protection systems that are used in rocket nozzles and re-entry bodies. These activities include the development, analysis, and testing of advanced materials in severe environments; as well as developing computational capabilities for computing the aerodynamic flow field, thermal protection system response, and thermal environment within the flight vehicle. Recent efforts have focused on developing a multi-dimensional finite element modeling capability to compute the thermal response within the ablator and interior of the vehicle. This presentation will present an overview of Sandias activities supporting development of thermal protection systems. An overview of Sandias numerical capabilities for computing the aerodynamic heating with equilibrium chemistry, the thermo- chemical ablator response, and the heat transfer into the vehicle will also be presented. These capabilities will be demonstrated for a prototypical example; the computed thermal response of a generic reentry body with aerodynamic heating representative of a typical flight profile.

Sandia is a multi-program laboratory operated by Sandia Corporation, a Lockheed Martin Company, for the United States Department of Energy under Contract DE-AC-04-94AL85000.

ABLATION TEST-CASES

Jean Lachaud, Alexandre Martin, Tom van Eekelen, Ioana Cozmuta

At the twilight of the Shuttle program, as announcements were made that planetary exploration would become one of NASA's top priorities, an area of research that had been mostly left untouched for 25 years experienced a notable resurgence: thermal protection system modeling. As researchers from academic institutions (re)-started working the problem, with the hope of modeling newly developed materials, or modeled heritage material with better accuracy and confidence, one thing quickly became clear: the models proposed were no better, if not inferior, than the one developed for the Apollo program. Two main reasons were identified to explain this trend: first, the ablative modeling expertise, not solicited for 25 years, had essentially been lost, and secondly, the data necessary to build those models was essentially inexistent, or protected under federal regulation, and therefore not available in the open literature. It became clear that if high-fidelity modeling tools, with predictive capabilities, were to be developed, those two issues would need to be addressed.

In an attempt to bring the community together, discuss new approaches, address issues, and present validating strategies, member of the federal agencies, academia and the industry tried to devise a project that would foment discussions. Such exercise had been quite successful in other communities, such as the *Current Zero Club*[**?**], for the study of electric arc interruption. Closer to the aerospace community, the well respected and widely attended *Drag Prediction Workshop*[**?**] had been immensely successful, and most of its objectives were the same as the ones identified to push ablation modeling further:

- assess the state-of-the-art computational methods
- provide an impartial forum for evaluating the effectiveness of existing computer codes and modeling techniques
- identify areas needing additional research and development
- promote balanced participation across academia, government labs, and industry.

Thus, it was decided that a similar exercise, using an ablative material test case, would be put together, and sent to all interested research groups.

The Ablation Workshop, sponsored by NASA, AFOSR and Sandia National Labs had been held since 2008, seemed like the perfect venue to carry out this plan. Moreover, for the 2011 edition, it was announced that, for the first time, the access would be unrestricted, and therefore freely open to academic institution as well as to the international community.

The first ablation test-case to the atmospheric re-entry community was therefore presented at the 4th NASA-AFOSR-SNL Ablation Workshop (1-3 March, 2011, Albuquerque, New Mexico). This first test-case was a simple heat transfer problem chosen for its simplicity. It included 14 participants - about 60% of the community. Code developers and users were really curious to see *how the codes would compare* and *what would be the effects of the different hypotheses in the models implemented*. Following this interest by the code developers, a second test-case series was presented at the 5th ablation workshop (Feb. 28-March 1, 2012, Lexington, Kentucky). The second test-case series went one step further, with the objective of reaching the state-of-the-art design level. It required the patience of the industrial participants for whom this second series still meant *running a basic case*, with codes that had already been tested, verified, and validated. It also required the comprehension of the academic participants for whom it implied implementing in their codes engineering models, with maybe no other intent than *running the second ablation test-case series* and comparing their codes with state-of-the-art design tools. It was agreed that problems of increasing complexity should be proposed until the most-elaborated well-defined problem has been formulated.

Ablation test-case series #3

- Numerical simulation of ablative-material response: code and model comparisons -

Tom van Eekelen * Alexandre Martin † Jean Lachaud ‡ Daniele Bianchi §

I. Introduction

Code developers and users are curious to see "how their code compares" and "what are the effects of the different hypotheses in the models implemented". In 2011, an effort was started to allow such comparisons for ablative material response codes and models, in an open forum. Since then, each year, a test-case series has been proposed within the framework of the NASA/AFOSR/SNL ablation workshop - around February, each year. This year, it is targeted to release the final version of the test-case in the timeframe of the 6^{th} *Ablation Workshop* at the University of Illinois (10-11 April 2014). The test-case series are designed to propose problems of increasing complexity. Each series tackles only a few aspects of the material response to allow a targeted comparison of the codes and of the models. The first test-case was mostly a heat transfer problem chosen for it's simplicity, allowing to set the focus on the in-depth material response (it is summarized in section A). The second test-case series went one step further and made use of a convective boundary condition - as in state-of-the-art design codes and reached the state-of-the-art (see section B). This document presents the third series. The main goal of this new series, is to test the 2D-axisymmetrical and 3D modeling capabilities of the participating codes and assess multidimensional effects. All tests within test-case series #3 re-use the TACOT material properties (but with an extended pressure and B'_g range) defined for the previous series.[2]

A. Summary of the first test-case

The first test case was defined for the 4^{th} *Ablation Workshop, 1-3 March 2011, Albuquerque, New Mexico*.[1] It is a one-dimensional test-case focusing on the in-depth material response - fixed surface temperature and no recession. Three types of material-response codes have been identified during this first comparison:

- Type 1: based on the CMA[4] model or any mathematically equivalent model (heat transfer, pyrolysis, simplified mass transport);
- Type 2: CMA-type + Averaged momentum equation for the transport of the pyrolysis gases;
- Type 3: Higher fidelity codes (chemical/thermal non-equilibrium, etc).

The results had been provided by the participants before the workshop and a summary was presented during the workshop.[3] For type 1 and type 2 codes, differences in the temperature prediction were mostly below 1%. Type-3 code results were more scattered but they were mostly based on heuristic models that will need further validation.

B. Summary of the second test-case series

The definition of the test case series #2 was finalized in January 2012.[2] The second test-case series aims at reaching the state-of-the-art TPS-design level. For consistency with test-case series #1 and to limit time-investment, most of the parameters and boundary conditions are unchanged. The main modifications are: (1) convective boundary condition (instead of fixed surface-temperature boundary condition), and (2)

*Tom.vanEekelen@lmsintl.com
†Alexandre.Martin@uky.edu
‡jlachaud@ucsc.edu
§Daniele.Bianchi@uniroma1.it

surface recession is allowed. Computing the ablation rate to obtain the amount of surface recession is a complicated and still open problem. A traditional B' table is provided to facilitate the in-depth material-response comparison but other tables/methods may be used. A specific test-case dedicated to the estimation of the ablation rate is also proposed. Therefore, the test-case series #2 includes three traditional ablation tests and one additional test dedicated to the estimation of the ablation rate:

- 2.1: low heating, no recession (targeted surface temperature of about 1644 K, cf. test-case 1) - non-physical intermediate case without recession in preparation for 2.2.
- 2.2: low heating (same as test case 2.1), recession
- 2.3: high heating, recession (targeted surface temperature of about 3000 K)
- 2.4: computation of the ablation rate of TACOT for a temperature range of 300K-4000K and an air pressure of 101325 Pa (1 atm). This is often referred to as 'B' table'.

Participants compared their results at the 5^{th} *Ablation Workshop, Lexington, Kentucky, Feb 28-March 1, 2013*. Results of type-1 and type-2 codes were in overall satisfactory agreement, with several codes (at least 5) featuring perfectly matching results for cases 2.1, 2.2 and 2.3. For case 2.4, slight differences have been seen: nothing that may be alarming for design purpose, but the community agreed that the results are significantly affected by the thermodynamics data used - and somehow by the algorithm used. A more refined and dedicated test-case may be needed in the future.

II. Description of the third test-case series

A preliminary version of the test cases of series #3 has been presented at the 5^{th} *Ablation Workshop, Feb. 28- March 1, 2012*. Since then some modifications have been made; for example, a test case concerning a small re-entry vehicle[5] has been removed. The selected test-cases consist of an "Iso-Q" sample submitted to typical arc-jet conditions .[6,7] A total of four tests - with an increasing level of multidimensionality - are proposed:

- 3.0: a 2D-axisymmetric model with an isotropic version of TACOT without ablation. This test is a non-physical test only meant to help code developers calibrate their codes before going into the model/code comparison. Results for all type-2 codes are expected to be identical.
- 3.1: the same test but including ablation - and therefore, recession.
- 3.2: the same test but with an orthotropic version of TACOT, aligned with the "Iso-Q" sample axis.
- 3.3: a full 3D model with an orthotropic version of TACOT, tilted by 30° compared to the "Iso-Q" sample axis.

III. The "Iso-Q" test-case; geometry and boundary conditions

The "Iso-Q" sample geometry and the boundary conditions are described in this section. The so-called "Iso-Q" samples, used in arc-jet test, unfortunately do not display a fully iso-flux contour.[8] This is particularly true for sphere-cylinder geometries often used for testing.[8] They display a strong heat flux augmentation at the shoulder. In this test-case series, we wish to run uncoupled material-CFD simulations. It is therefore critical to use an initial shape with a more aero-thermodynamical profile, featuring a minimal heat flux augmentation at the shoulder. The idea is that even when running uncoupled simulations, the initial shape of the sample - and therefore the heat flux profile - should be conserved over time; that is, the ablation should be almost constant over most of the sample surface. A the same time, the initial geometry should be simple enough to ease the mesh generation - as participants do not necessarily have a lot of time to run the test-case series. Ellipse-cylinder geometries are good candidates as they allow the definition of continuous curvatures and are simple to define.

A. Geometry of the "Iso-Q" ellipse-cylinder sample

Current "Iso-Q" sphere-cylinder samples are often chosen with a sphere curvature radius equal to the diameter of the cylinder, as shown in figure 1. It was decided to use an ellipsoid instead of a sphere with a geometry as close as possible to state-of-the-art samples. In other words, a 2D axisymmetrical projection, where the circle-arc and the small (D/16) shoulder radius will be replaced by a single ellipse arc, as shown in figure 2. The geometry of the modified "Iso-Q" specimen is then an ellipse on top of a cylinder. The cylinder has a radius of $R_{cyl} = 50$ mm, and the ellipse a major axis of $R_e = 50$ mm and a minor axis of $r_e = R(2 - \sqrt{3}) = 13.397$ mm. The dimensions are reproduced in Figure 2.

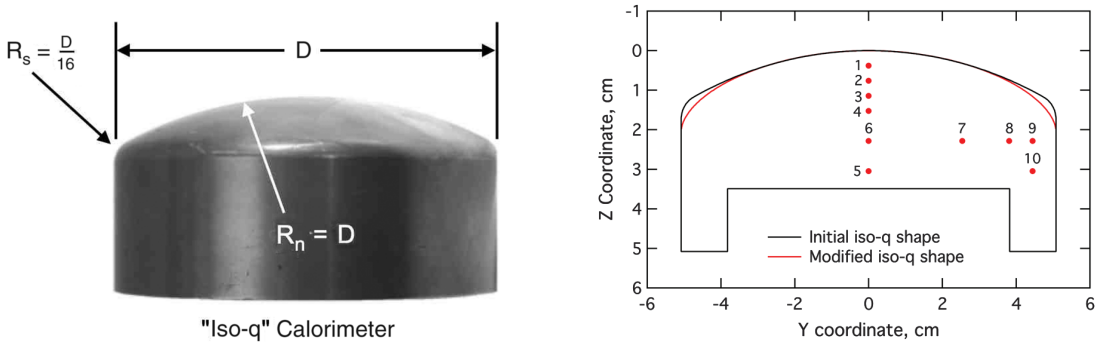

(a) "Iso-Q" test specimen

(b) position of the thermo-couples

Figure 1. State-of-the-art sample geometry and thermocouple placement.[6–8] NOTE: thermocouple placement is re-used but the geometry is slightly modified for the test-case series (see figure 2)

In Figure 1(b) and Table 1 we see the position of the thermo-couples, for which the temperature evolutions will be post-processed.

Table 1. Coordinates of the thermo-couples.

TC	Y-coordinate [cm]	Z-coordinate [cm]	TC	Y-coordinate [cm]	Z-coordinate [cm]
1	0.00	0.381	6	0.00	2.286
2	0.00	0.762	7	2.540	2.286
3	0.00	1.143	8	3.810	2.286
4	0.00	1.524	9	4.445	2.286
5	0.00	3.048	10	4.445	3.048

All the thermocouples are placed in the sample plane (x=0). This might not be ideal practice for a real sample but, here, it will greatly simplify the response post-processing for test 3.3.

"Iso-Q" test specimens include a support structure added to the geometry shown in Figure 1(b). Although the support structure will in general be made of a different material, here we will assume it is also made of TACOT for the simplicity of the analysis. Also, the contact between the "Iso-Q" sample and the support structure is assumed to be perfect. In other words, the example can be treated as a single block of TACOT. It is therefore allowed to create one continuous mesh/discretization for the "Iso-Q" and the support structure.

Please contact us if you find the definition unclear on incomplete. We will be happy to update the document accordingly.

B. Boundary conditions

The test-specimen is subjected to a similar heat load as applied in test 2.3 of test-case series #2. The specimen is subjected to a convective boundary condition. The sample is heated for 40 seconds, and it is let to cool-down for 1 minute by radiation cooling. The initial conditions are a uniform pressure and temperature: $p_0 = 0.004$ atm. (405.3 Pa), $T_0 = 300$ K. The initial gas composition in the material is left open. For type 1 and 2 codes, pyrolysis gas in thermal equilibrium is the usual practice. For type 3 codes,

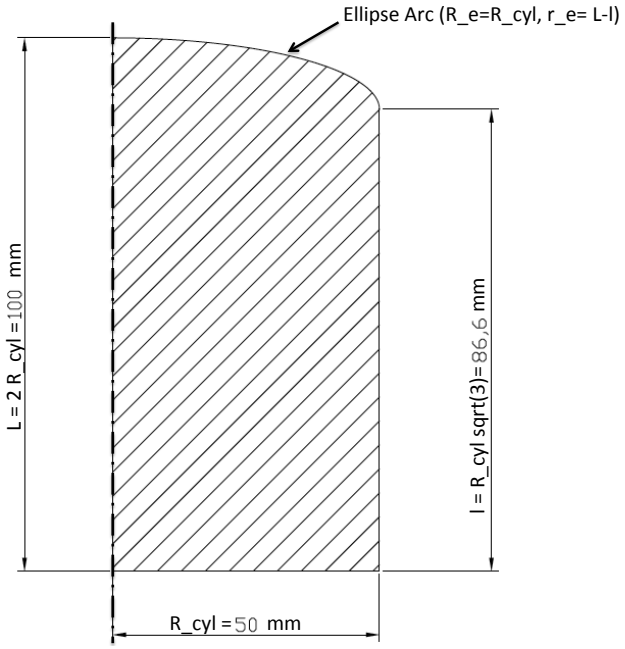

Figure 2. Geometry and dimensions of the "Iso-Q" specimen (in mm).

Table 2. Summary of the environment properties. Please use linear interpolation during the 0.1s heating and cooling periods (linear ramping).

time (s)	$\rho_e u_e C_h(0)$ (kg· m^{-2}· s^{-1})	h_e (J· kg^{-1})	$p_w(0,t)$ (Pa)	$p_w(11.17,t)$ (Pa)
0	$0.1 \cdot 10^{-2}$	0	405.3	405.3
0.1	0.1	$2.5 \cdot 10^7$	10132.5	405.3
40	0.1	$2.5 \cdot 10^7$	10132.5	405.3
40.1	$0.1 \cdot 10^{-2}$	0	405.3	405.3
120	$0.1 \cdot 10^{-2}$	0	405.3	405.3

it is suggested to start with air. The time-dependent boundary-layer properties at the stagnation point are summarized in table 2. The other boundary-layer assumptions/properties are as follows for the code comparison:

- The factor for the blowing-correction correlation, used in the CMA model, is taken as $\lambda = 0.5$.
- Heat and mass transfer assumptions in the boundary layer: $Pr = Le = 1$
- Re-radiation is active during the entire analysis [$q_r = \epsilon\sigma(T_w^4 - T_\infty^4)$]. Due to the convex shape of the test-specimens, a view factor of 1 is used. The infinity temperature is chosen to be $T_\infty = 300$ K .
- Use the wall enthalpy (h_w) and the B'_c table provided in the TACOT_3.0.xls file for code comparison.

The heat transfer coefficient and pressure profiles over the ellipsoid geometry have been estimated using a non-equilibrium aerothermodynamic hypersonic CFD code.[10] The free stream conditions used in this calculation are for air at a temperature of 225 K, at a density of 2.3×10^{-3} kg/m^3, traveling at 7000 m/s. A super-catalytic wall is used, at a temperature of 225 K.

For this test-case we will thus apply the heat-flux and pressure profile defined in Figure 3, where we pre-multiply $\rho_e u_e C_h(0)$ with the $q_w/q_w(0)$ values in Table 3. For the pressure it is slightly more complicated. At time $t = 0$ the pressure profile on the outer surface will be uniform ($p_w = 405.3$ Pa). During 0.1 seconds

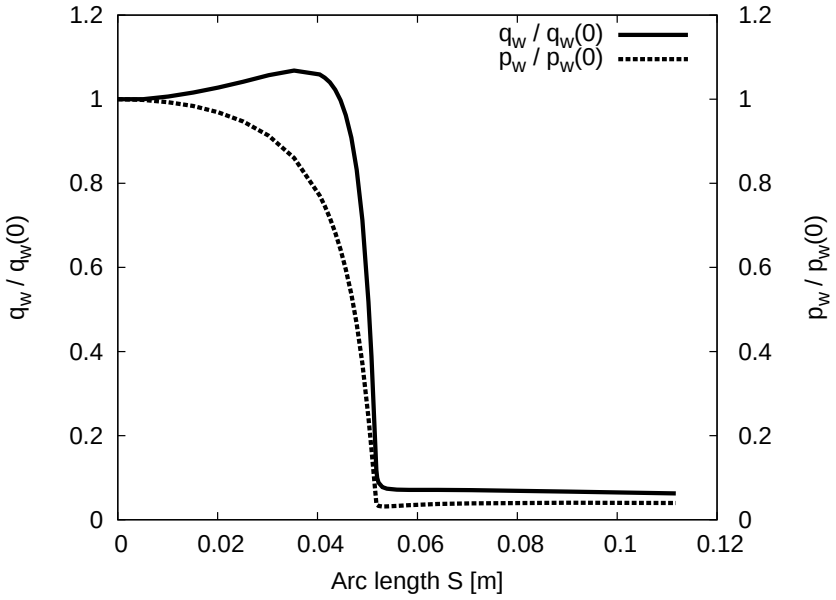

Figure 3. Heat flux and pressure distributions for the "Iso-Q" specimen.

Table 3. Distribution of the $q_w/q_w(0)$ values as a function of the Y- and Z-coordinate (plotted in Figure 3). In computations, please let vary the heat transfer coefficient (Ch), but not the edge enthalpy.

s (cm)	Y (cm)	Z (cm)	$q_w/q_w(0)$	$p_w/p_w(0)$	s (cm)	Y (cm)	Z (cm)	$q_w/q_w(0)$	$p_w/p_w(0)$
0.00	0.000	0.000	1.000	1.000	4.78	4.701	-0.884	0.833	0.466
0.51	0.507	-0.007	1.000	0.998	4.90	4.802	-0.967	0.712	0.371
1.01	1.008	-0.028	1.006	0.993	5.02	4.903	-1.078	0.518	0.243
1.51	1.509	-0.062	1.016	0.984	5.08	4.949	-1.149	0.388	0.167
2.01	2.008	-0.113	1.028	0.969	5.18	5.000	-1.348	0.118	0.039
2.51	2.505	-0.180	1.042	0.947	5.20	5.000	-1.411	0.100	0.035
3.02	3.009	-0.270	1.057	0.913	5.22	5.000	-1.505	0.088	0.033
3.53	3.508	-0.385	1.068	0.860	5.30	5.000	-1.757	0.078	0.031
4.04	4.007	-0.538	1.059	0.771	5.39	5.000	-2.009	0.074	0.032
4.15	4.105	-0.575	1.051	0.746	5.59	5.000	-2.497	0.071	0.033
4.25	4.202	-0.614	1.040	0.718	5.83	5.000	-3.001	0.071	0.035
4.35	4.304	-0.658	1.023	0.683	6.41	5.000	-4.009	0.071	0.038
4.46	4.405	-0.706	0.998	0.643	7.07	5.000	-5.001	0.070	0.039
4.57	4.503	-0.757	0.962	0.596	9.02	5.000	-7.504	0.067	0.040
4.68	4.604	-0.817	0.909	0.536	11.17	5.000	-9.992	0.063	0.040

the pressure is increased (decreased for $5.18 \leq s \leq 7.07$) to $10132.5 \times p_w/p_w(0)$, using the pressure profile of Table 3. This pressure profile will be held constant until $t = 40.$ seconds. After this period, the surface pressure will be linearly reduced (during 0.1 seconds) to the initial uniform pressure of 405.3 Pa. At the stagnation point and the base this results in the time variation $p_w(s,t)$ given in Table 2.

We will use the TACOT wall enthalpy h_w and ablation rate B'_c values, obtained for different pressure values p_w between 0.001 and 1.0 atm. The back-side of the support structure is considered to be an adiabatic and impermeable wall.

IV. Test-case definitions

A total of four test-cases are defined, each one with an increasing complexity to go continuously from the series #2 test-cases to a general an-isotropic 3D test-case.

1. Model with an isotropic material (Tests 3.0 and 3.1)

Two test-cases will be run with isotropic material properties, namely:

- 3.0: a 2D-axisymmetric model with an isotropic version of TACOT without ablation, as in test-case 2.1 (h_w is read from the $B_c^{'}$ table but $B_c^{'}$ is artificially taken equal to zero). This test is a non-physical test only meant to help code developers calibrate their codes before going into the model/code comparison, and may be skipped. Results for all type-2 codes are expected to be identical.
- 3.1: the same test but including ablation - and therefore, recession.

2. Model with an orthotropic material (Test 3.2)

One of the goals of this test-series, is to compare the modeling capabilities of the different codes. One of the modeling capabilities, of practical interest, is to model orthotropic materials. For example PICA[6] is known to be orthotropic, where the through-the-thickness conductivity is lower that the isotropic conductivity, and the in-plane conductivity is higher than the isotropic conductivity. We therefore propose to use an orthotropic model, where the conductivities are defined via multiplication factors ($\alpha_1 = 1.0, \alpha_2 = 2.0$) for the isotropic conductivity of the TACOT model.

$$\begin{vmatrix} \lambda_{TTT} & 0 \\ 0 & \lambda_{IP} \end{vmatrix} = \begin{vmatrix} \alpha_1 & 0 \\ 0 & \alpha_2 \end{vmatrix} \lambda_{\text{isotropic}} \tag{1}$$

The through the thickness direction is aligned with the axis of axis-symmetry (Z-axis in Figure 1).

A. A full 3D model with an orthotropic material (Test 3.3)

A final functionality that will be tested within series #3, is the full 3D modeling capabilities of the participating codes. The full 3D test will be a simple extension of the orthotropic material test of section 2. For this test, the through-the-thickness direction will form an angle $\alpha = 30°$ (positive in the counter clock-wise direction) with the axis of axis-symmetry in the x=0 plane (see Figure 4). This configuration will lead to a

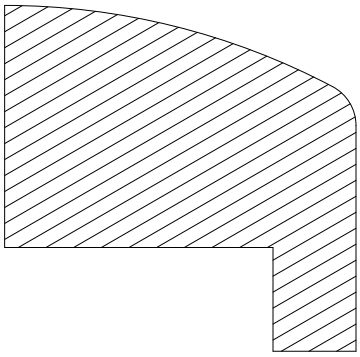

Figure 4. Visualization of the in-plane orientation.

full 3D problem with 3D heat and gas mass flow.

V. Material data

New thermochemical material properties have been generated for this test-case series. This was necessary because the pressure level of the test-case has been reduced, and the original data was only available at

$p = 1.0$ atm. The material properties for this test-case series are provided and explained in the spreadsheet TACOT_3.0.xls. The pyrolysis gas properties are generated as a function of temperature for three different values of the pressure ($p = 0.01, 0.1$ and 1.0 atm.). In Figure 5 the H_w and B'_c tables as a function of temperature is given for two values of the pressure (four values are calculated $p = 0.001, 0.01, 0.1$ and 1.0 atm.) and 25 values of B'_g.

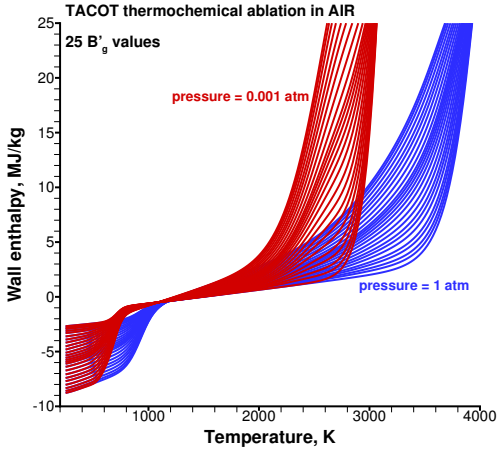

(a) H_w as a function of temperature and B'_g

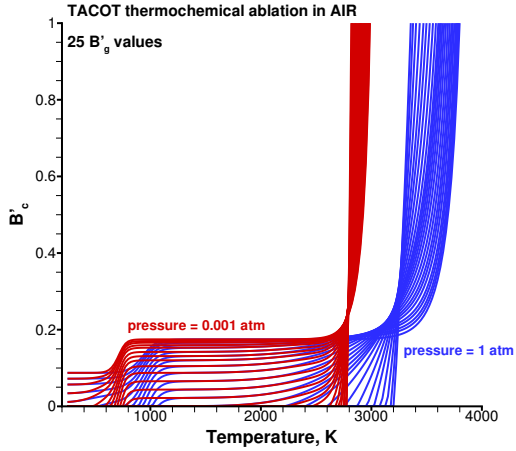

(b) B'_c as a function of temperature and B'_g

Figure 5. TACOT thermchemical ablation in AIR for different values of the pressure, using the TARGET[11] code.

The assumptions made, in order to get the new thermochemical values for TACOT, are the same as the ones made for version 2.2. Namely that an equilibrium calculation is performed, and that no condensed species are allowed to form in the mixture. The values are obtained with the TARGET[11] code (**T**hermochemical **A**blation **R**outine for the **G**eneration of **E**quilibrium **T**ables), which uses the CEA material data-base.

VI. Code output and comparison of the results

The results will be supplied in ASCII file format, which contain the following results (with an output frequency of $0.1\,s$):

- The temperature at the position of the stagnation point and of the 10 thermo-couples will be post-processed. The position of the thermo-couples are defined in Table 1 and Figure 1.
- For the same points (stagnation point and the thermo-couples) also the pressure and the density will be post-processed.

Output format desired:

time (s)	Tw (K)	T1 (K)	T2 (K)	T3 (K)	...	T8 (K)	T9 (K)	T10 (K)
0	3.000e2	3.000e2	3.000e2	3.000e2	3.000e2	3.000e2	3.000e2	3.000e2
0.1	9.651e2	3.225e2	3.000e2	3.000e2	3.000e2	3.000e2	3.000e2	3.000e2
0.2	1.076e3	3.956e2	3.039e2	3.000e2	3.000e2	3.000e2	3.000e2	3.000e2
etc.	...	...	...	...	...	...	...	...

Table 4. Output format for the temperature file: CodeName_Energy_TestCase_3-i.txt

It is more convenient to generate separate result files for the four test cases of section III. We propose to use indices in the file names, where the i in the file names will refer to:

time (s)	Pw (N/m2)	P1 (N/m2)	P2 (N/m2)	...	P10 (N/m2)
0	1.01325e4	1.01352e4	1.01352e4	1.01352e4	1.01352e4
0.1	1.01325e4	1.01352e4	1.01352e4	1.01352e4	1.01352e4
0.2	1.01325e4	1.01352e4	1.01352e4	1.01352e4	1.01352e4
etc.	...	...	...	...	...

Table 5. Output format for the pressure file: CodeName_Pressure_TestCase_3-i.txt

time (s)	rhow (kg/m3)	rho1 (kg/m3)	rho2 (kg/m3)	...	rho10 (kg/m3)
0	2.800e2	2.800e2	2.800e2	2.800e2	2.800e2
0.1	2.7900e2	2.800e2	2.800e2	2.800e2	2.800e2
0.2	2.7500e2	2.800e2	2.800e2	2.800e2	2.800e2
etc.	...	...	...	...	...

Table 6. Output format for the density file: CodeName_Density_TestCase_3-i.txt

- $i = 0$: Model with an isotropic material but without surface recession,
- $i = 1$: Model with an isotropic material,
- $i = 2$: Model with an orthotropic material,
- $i = 3$: A full 3D model with an orthotropic material.

VII. Preliminary results

In previous versions of the test-case, the pressure at the outer surface was held constant, due to an un-physical temperature drop at the beginning of the analysis. Because of the change in pressure values, the initial gas mass flow is smaller and so is the cooldown due to the negative value (equilibrium assumption of the pyrolysis gas) of the third term on the right hand side in the next equation:

$$q_i n_i = \rho_e u_e C_h \left[(h_e - h_w) + B'_c (h_c - h_w) + B'_g (h_g - h_w) \right] \tag{2}$$

Here the pressure distribution of Figure 3 is used. In order to start the transient analysis from an equilibrium solution the initial pressure distribution inside the test-specimen is calculated at time $t = 0$ seconds.

Besides the thermo-couple results, that need to be supplied for comparisons, additional results will be given in the annex of this report. These additional results will be helpful in identifying any problems that might arise when comparing the results of the different codes.

The results shown are generated with SAMCEF Amaryllis. Please do not give them more credit than they deserve and use them for sanity check rather than for comparison. In test-case 3.3 (numerical) oscillations were obtained in the temperature at the wall. The cause of these oscillations has not yet been identified. In all test-cases we see a (numerical) non-smooth pressure evolution during the cool-down phase. The cause for this behavior had not yet been identified.

Acknowledgments

We would like to thank you in advance for any comment that will help to improve the clarity of this document. Please send your comments to the authors.

References

[1]Lachaud, J., Martin, A., Cozmuta, I., and Laub, B., "Ablation Workshop Test Case - Version 1.1 - Feb. 2, 2011," Prepared for the 4^{th} Ablation Workshop (1-3 March 2011. Albequerque, New Mexico).

[2]Lachaud, J., Martin, A., van Eekelen, T., and Cozmuta, I., "Ablation test-case series #2 - Version 2.8 - Feb. 6, 2012," Prepared for the 5th Ablation Workshop (28 February - 1 March 2012. Lexington, Kentucky).

[3]"Overview of Intercalibration Results," Thermal Performance Database Team, Oral presentation, 4th Ablation Workshop (1-3 March 2011. Albequerque, New Mexico).

[4]Kendall, R. M., Bartlett, E. P., Rindal, R. A., and Moyer, C. B., "An Analysis of the Coupled Chemically Reacting Boundary Layer and Charring Ablator," Contractor report CR-1060, NASA, 1968.

[5]Empey, D. M., Skokova, K. A., Agrawal, P., Swanson, G. T., Prabhu, D. K., Peterson, K. H., and Venkatapathy, E., "Small Probe Reentry Investigation for TPS Engineering (SPRITE)," 8th *International Planetary Probe Workshop*, IPPW-8, Portsmouth, Virginia, 2011.

[6]Milos, F. and Chen, Y.-K., "Two-Dimensional Ablation, Thermal Response, and Sizing Program for Pyrolyzing Ablators," *Journal of Spacecraft and Rockets*, Vol. 46, No. 6, December 2009, pp. 1089–1099.

[7]Agrawal, P., Ellerby, D. T., Switzer, M. R., and Squire, T. H., "Multidimensional Testing of Thermal Protection Materials in the Arcjet Test Facility," 10th *AIAA/ASME Joint Thermophysics and Heat Transfer Conference*, No. AIAA 2010-4664, AIAA, 2010.

[8]Milos, F. and Chen, Y.-K., "Ablation and Thermal Response Property Model Validation for Phenolic Impregnated Carbon Ablator," *Journal of Spacecraft and Rockets*, Vol. 47, No. 5, September-October 2010, pp. 786–805.

[9]Dec, J. A., Laub, B., and Braun, R. D., "Two-Dimensional Finite Element Ablative Thermal Response Analysis of an Arcjet Stagnation Test," 42nd *AIAA Thermophysics Conference*, No. AIAA 2011-3617, 27-30 June 2011.

[10]Martin, A., Scalabrin, L. C., and Boyd, I. D., "High performance modeling of an atmospheric re-entry vehicle," *Journal of Physics: Conference Series*, Vol. 341, 2012, pp. 1013.

[11]Bianchi, D., "A CEA-based Chemical Equilibrium Solver for Gas/Surface Thermochemistry and Thermochemical Tables Generation," *Centro Ricerca Aerospaziale Sapienza (CRAS),* Contract Reference no. CRAS-TTG-1001, Sapienza University of Rome, 2013.

Results of the test case series#3

2D and 3D finite element mesh

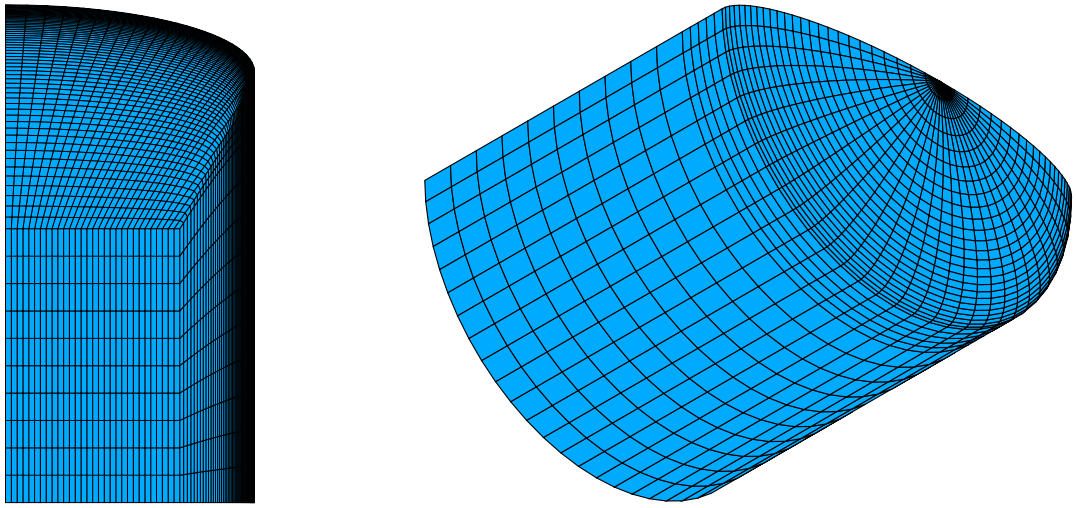

(a) 2D-mesh (b) 3D-mesh

Figure 6. Un-deformed finite element mesh.

Miscellaneous results for test-case 3.1, 3.2 and 3.3

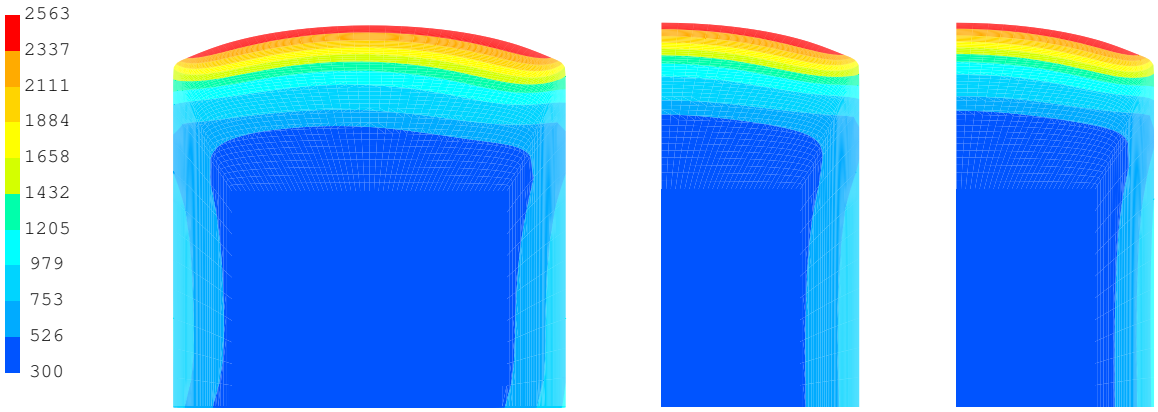

(a) Test-case 3.3 (b) Test-case 3.2 (c) Test-case 3.1

Figure 7. Temperature [K] distribution on a deformed structure at time t=39 seconds.

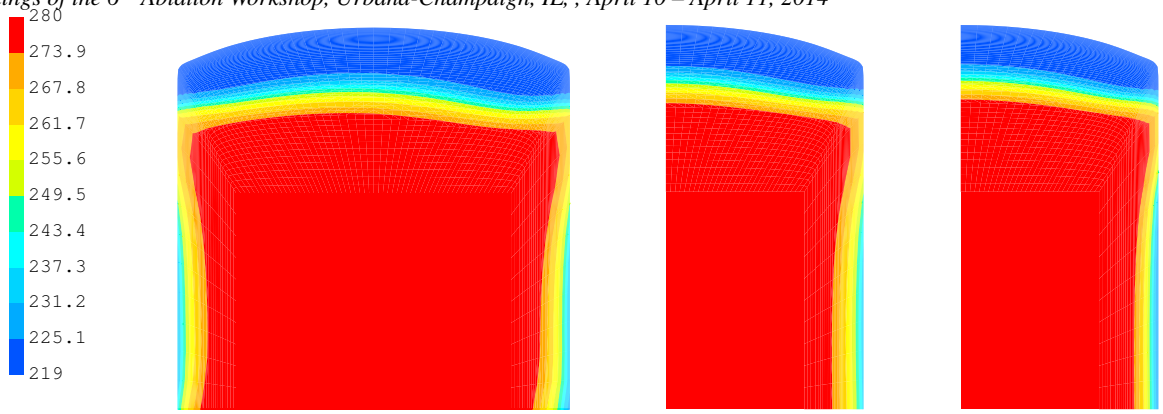

(a) Test-case 3.3 (b) Test-case 3.2 (c) Test-case 3.1

Figure 8. Density [kg/m^3] distribution on a deformed structure at time t=39 seconds.

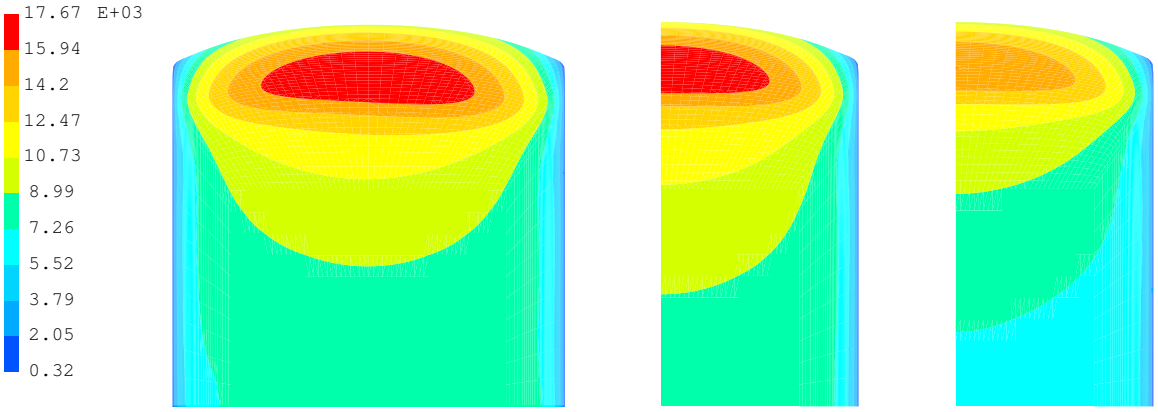

(a) Test-case 3.3 (b) Test-case 3.2 (c) Test-case 3.1

Figure 9. Pressure [N/m^2] distribution on a deformed structure at time t=39 seconds.

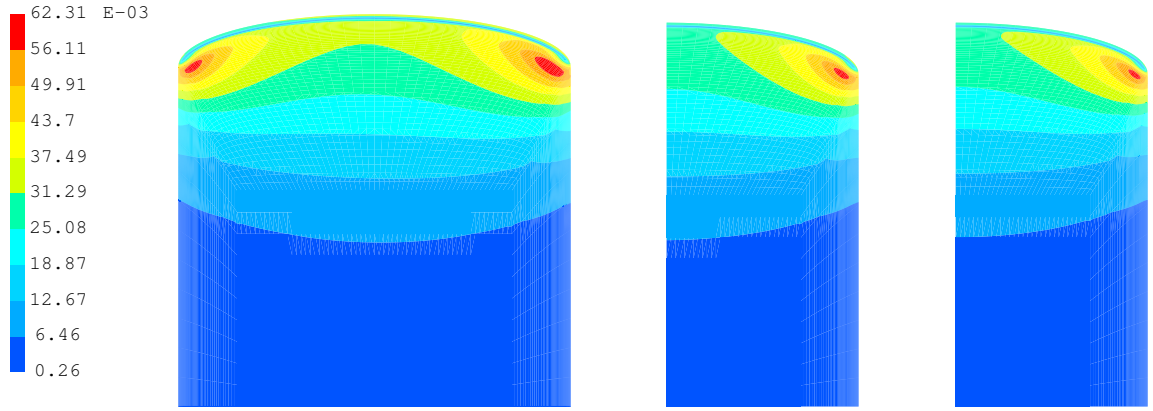

(a) Test-case 3.3 (b) Test-case 3.2 (c) Test-case 3.1

Figure 10. Gas mass flow [kg/(m^2.s)] distribution on a deformed structure at time t=0.8 seconds.

Surface results for test-case 3.0, 3.1, 3.2 and 3.3

The gas mass flow results given in the following figures is the modulus of the gas mass flow vector, i.e. this vector is not necessarily perpendicular to the outer surface.

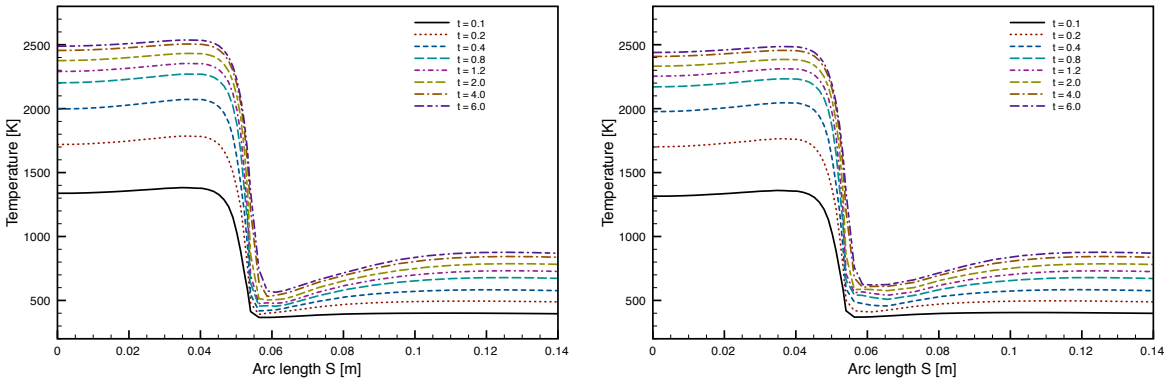

(a) Test-case 3.0 (b) Test-case 3.1

Figure 11. Temperature along the outer surface at different time instances.

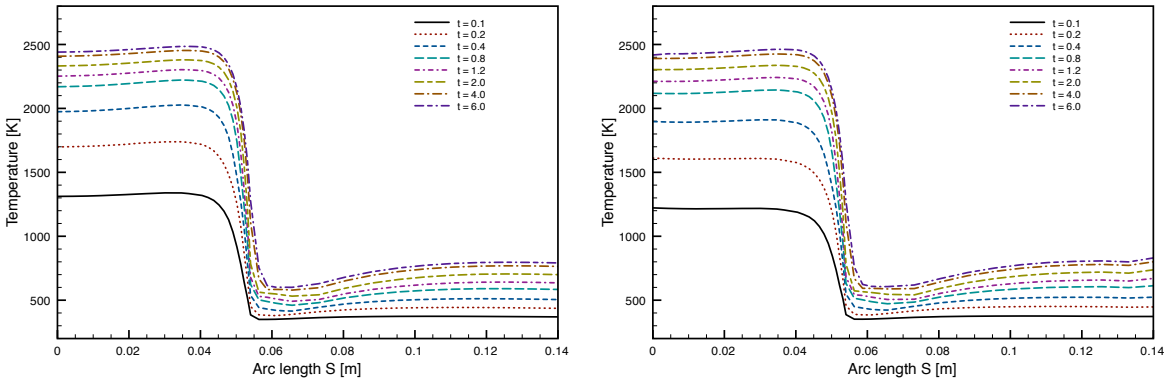

(a) Test-case 3.2 (b) Test-case 3.3

Figure 12. Temperature along the outer surface at different time instances.

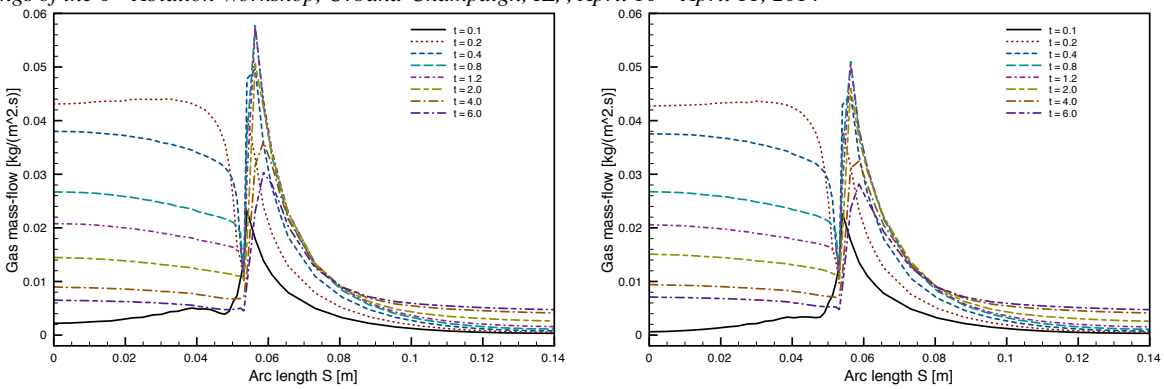

(a) Test-case 3.0 (b) Test-case 3.1

Figure 13. Modulus of the gas mass-flow along the outer surface at different time instances.

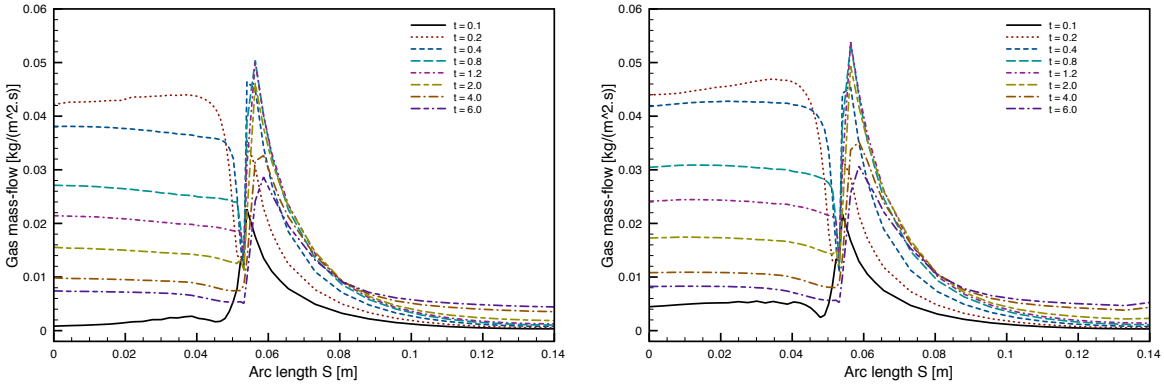

(a) Test-case 3.2 (b) Test-case 3.3

Figure 14. Modulus of the gas mass-flow along the outer surface at different time instances.

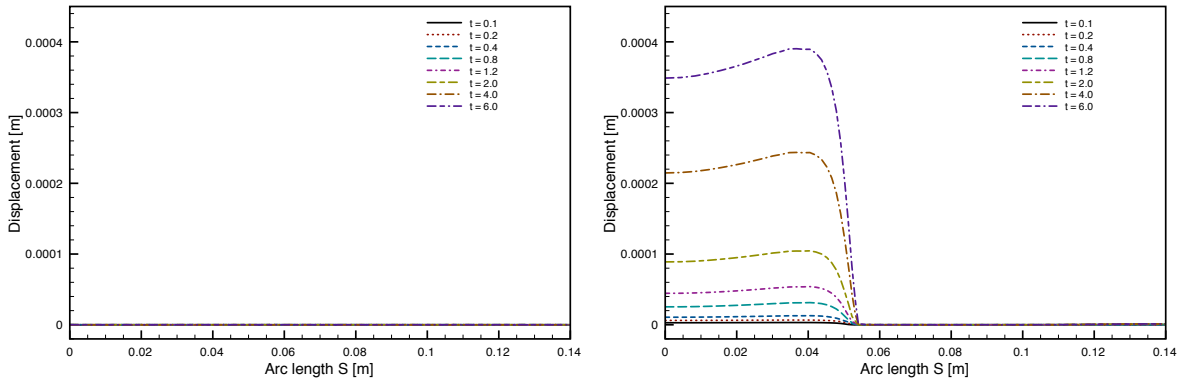

(a) Test-case 3.0 (b) Test-case 3.1

Figure 15. Modulus of the ablation deformation along the outer surface at different time instances.

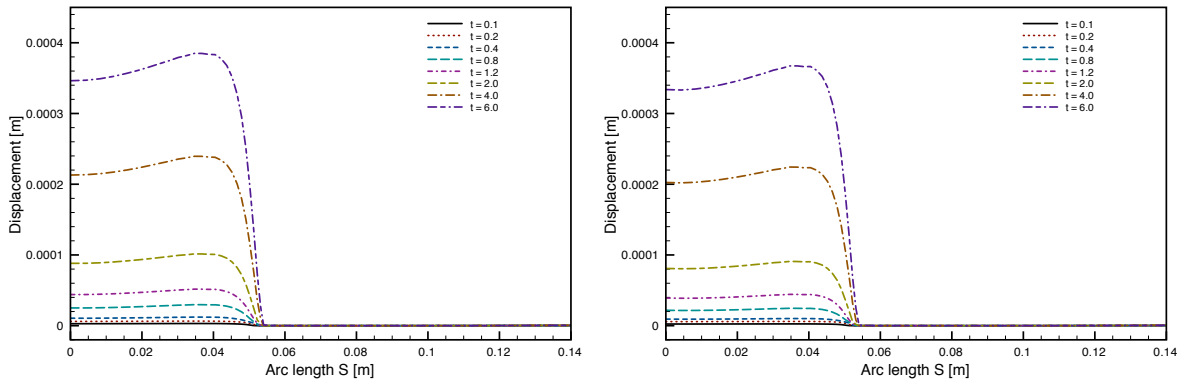

(a) Test-case 3.2 (b) Test-case 3.3

Figure 16. Modulus of the ablation deformation along the outer surface at different time instances.

Temperature curves for test-case 3.0, 3.1 and 3.2

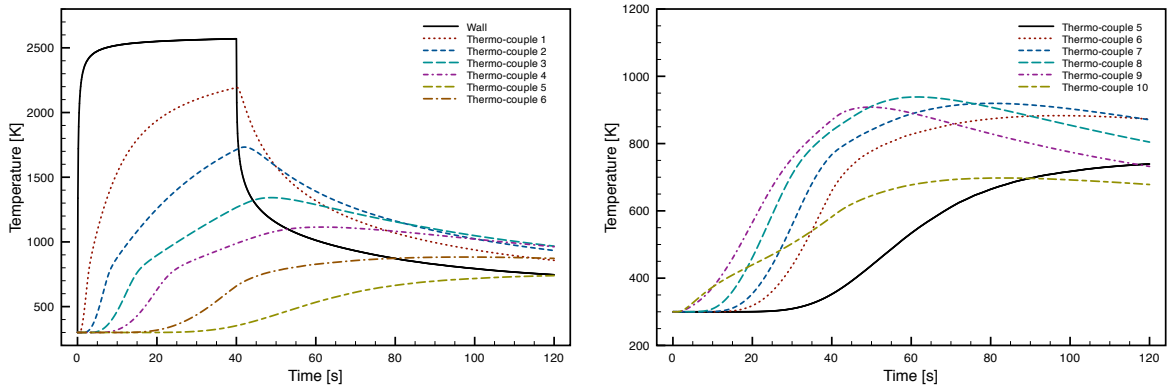

(a) thermo-couples 1 till 6 (b) thermo-couples 5 till 10

Figure 17. Temperature evolution of the wall and the thermo-couples for Test 3.0.

Pressure curves for test-case 3.0, 3.1 and 3.2

Density curves for test-case 3.0, 3.1 and 3.2

Comparison of temperature curves for test-case 3.2 and 3.3

In test-case 3.3 (numerical) oscillations were obtained in the temperature at the wall. The cause of these oscillations has not yet been identified.

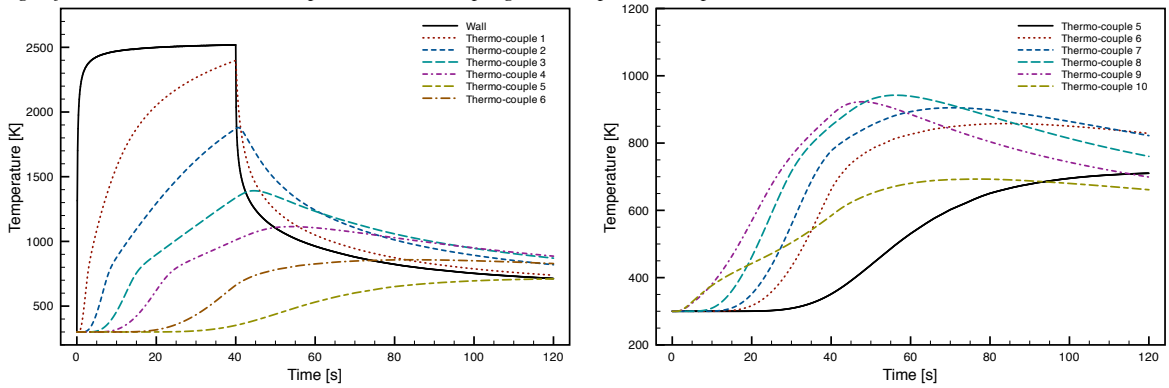

(a) thermo-couples 1 till 6 (b) thermo-couples 5 till 10

Figure 18. Temperature evolution of the wall and the thermo-couples for Test 3.1.

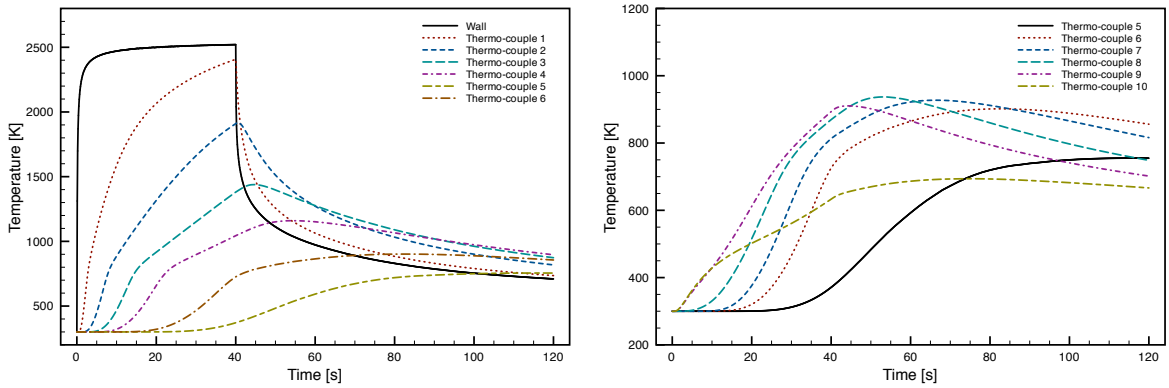

(a) thermo-couples 1 till 6 (b) thermo-couples 5 till 10

Figure 19. Temperature evolution of the wall and the thermo-couples for Test 3.2.

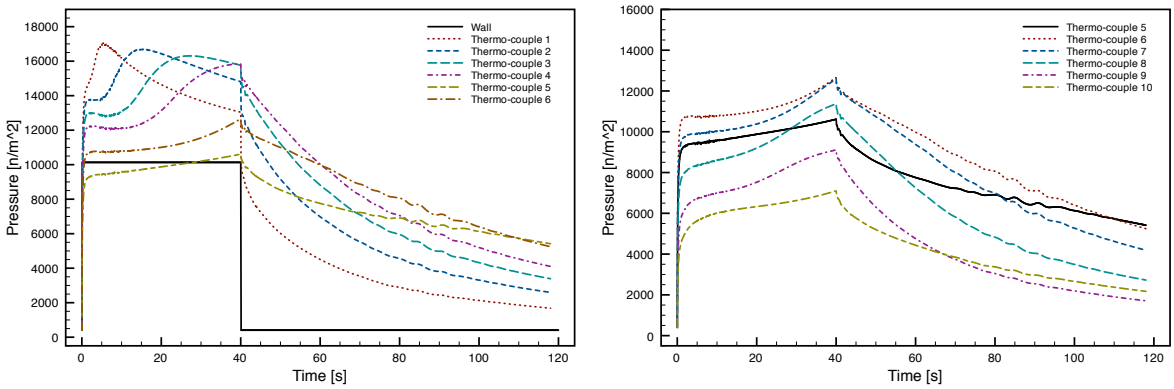

(a) thermo-couples 1 till 6 (b) thermo-couples 5 till 10

Figure 20. Pressure evolution of the wall and the thermo-couples for Test 3.0.

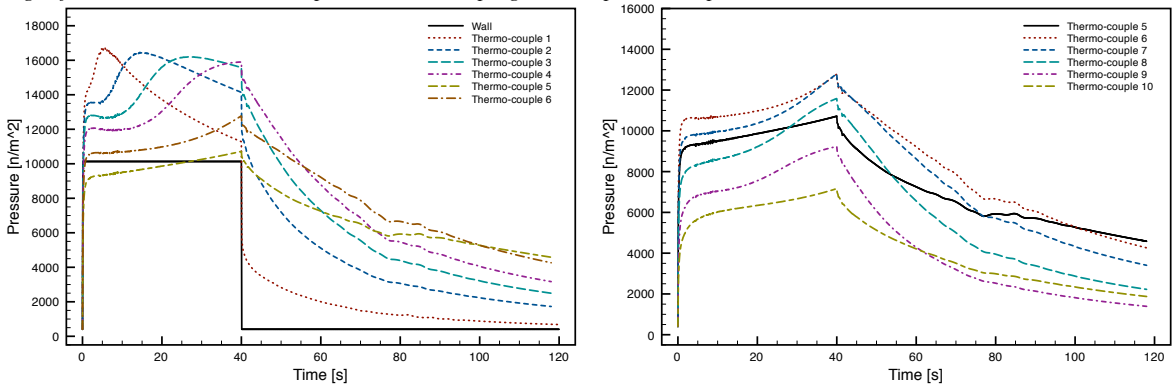

(a) thermo-couples 1 till 6 (b) thermo-couples 5 till 10

Figure 21. Pressure evolution of the wall and the thermo-couples for Test 3.1.

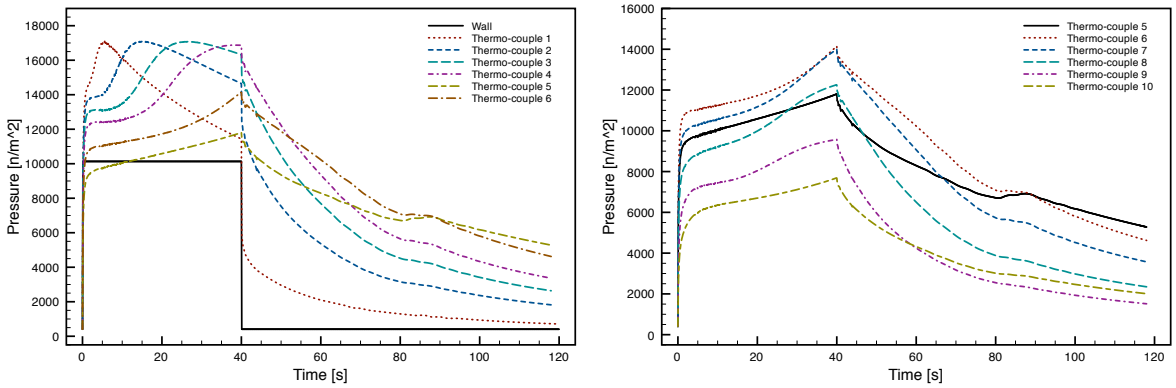

(a) thermo-couples 1 till 6 (b) thermo-couples 5 till 10

Figure 22. Pressure evolution of the wall and the thermo-couples for Test 3.2.

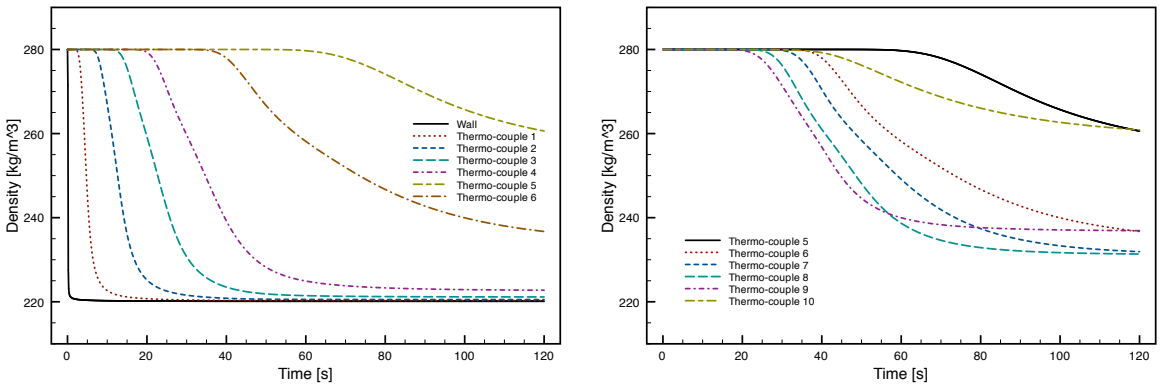

(a) thermo-couples 1 till 6 (b) thermo-couples 5 till 10

Figure 23. Density evolution of the wall and the thermo-couples for Test 3.0.

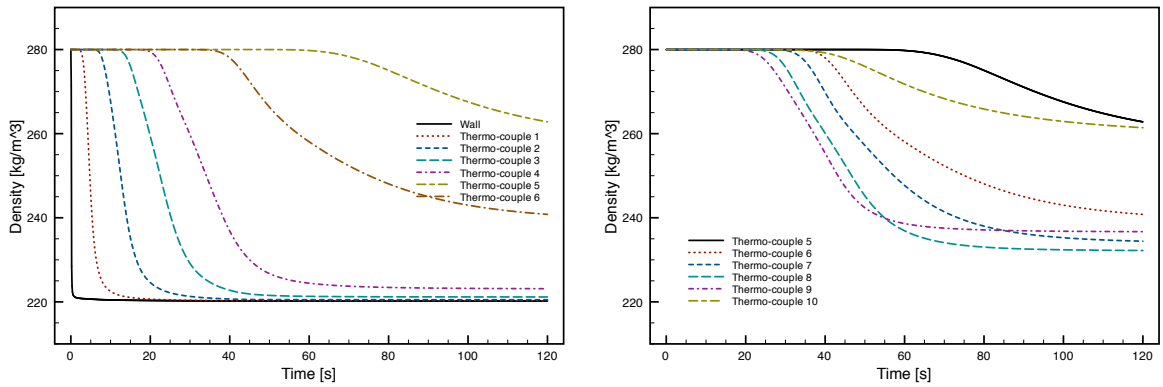

(a) thermo-couples 1 till 6 (b) thermo-couples 5 till 10

Figure 24. Density evolution of the wall and the thermo-couples for Test 3.1.

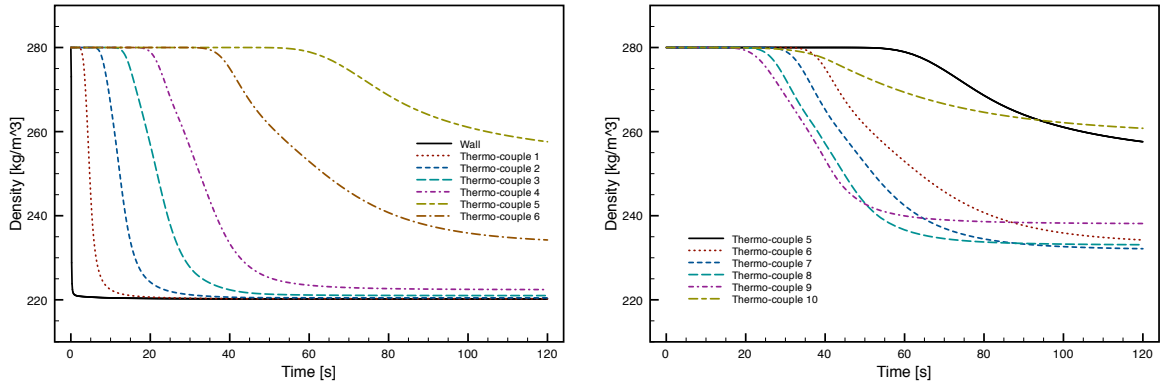

(a) thermo-couples 1 till 6 (b) thermo-couples 5 till 10

Figure 25. Density evolution of the wall and the thermo-couples for Test 3.2.

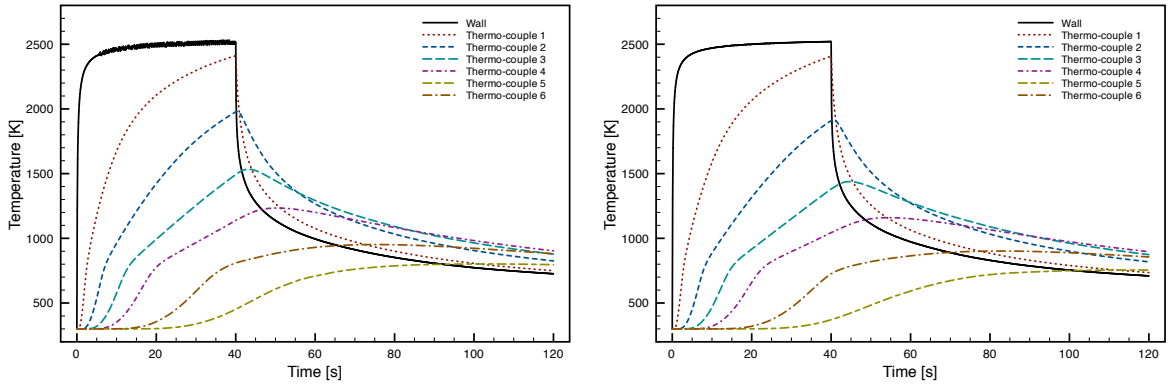

(a) Test 3.3 (b) Test 3.2

Figure 26. Temperature evolution of the wall end the thermo-couples 1 till 6.

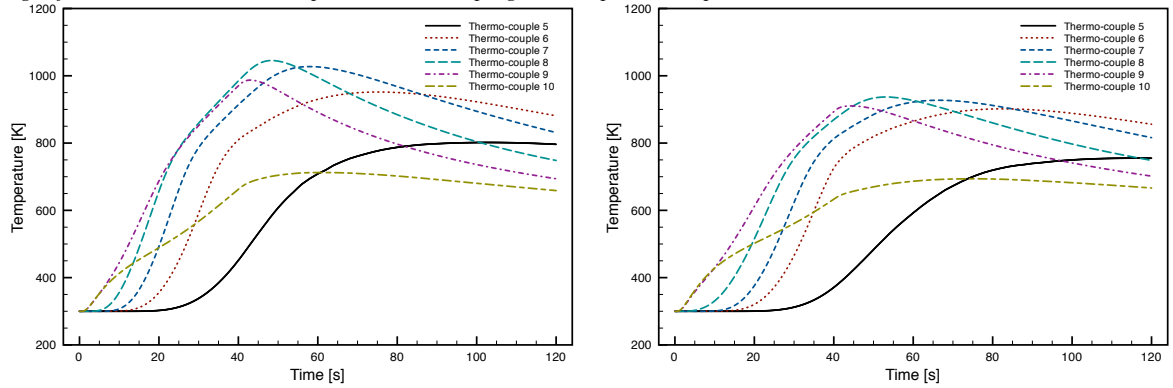

(a) Test 3.3 (b) Test 3.2

Figure 27. Temperature evolution of the thermo-couples 5 till 10.

Comparison of pressure curves for test-case 3.2 and 3.3

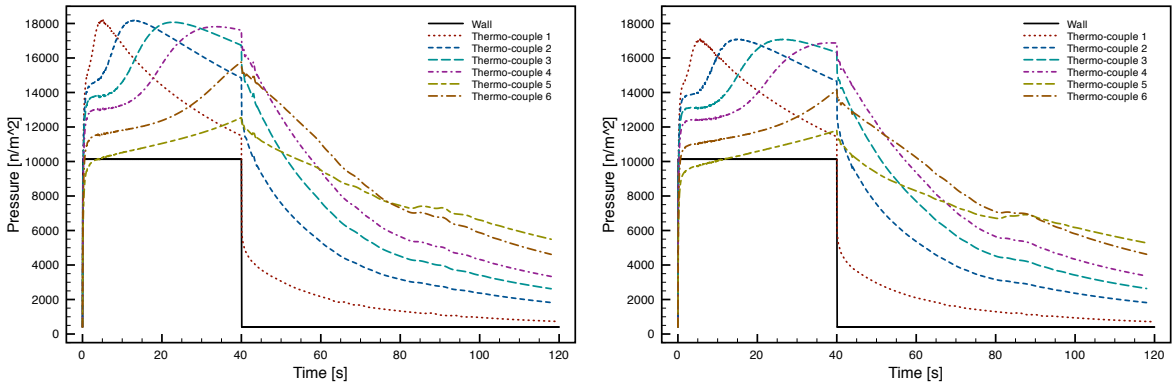

(a) Test 3.3 (b) Test 3.2

Figure 28. Pressure evolution of the wall and the thermo-couples 1 till 6.

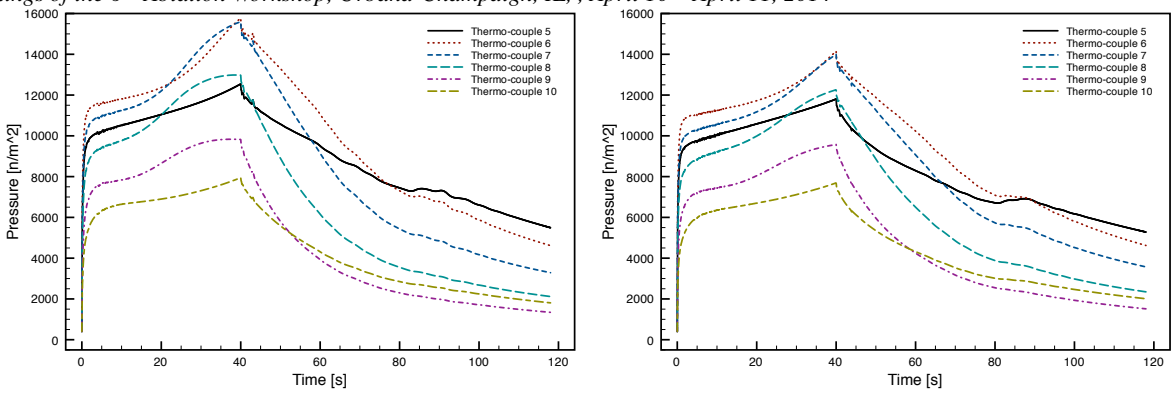

(a) Test 3.3 (b) Test 3.2

Figure 29. Pressure evolution of the thermo-couples 5 till 10.

Comparison of density curves for test-case 3.2 and 3.3

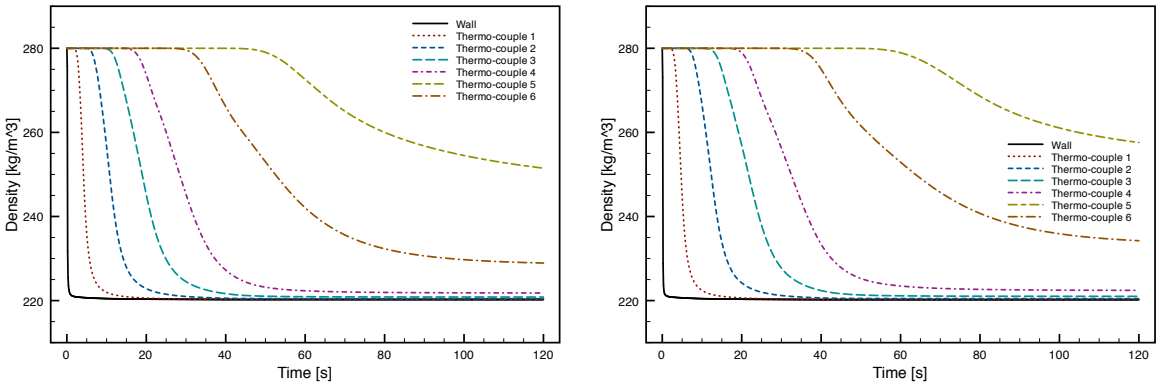

(a) Test 3.3 (b) Test 3.2

Figure 30. Density evolution of the wall and the thermo-couples 1 till 6.

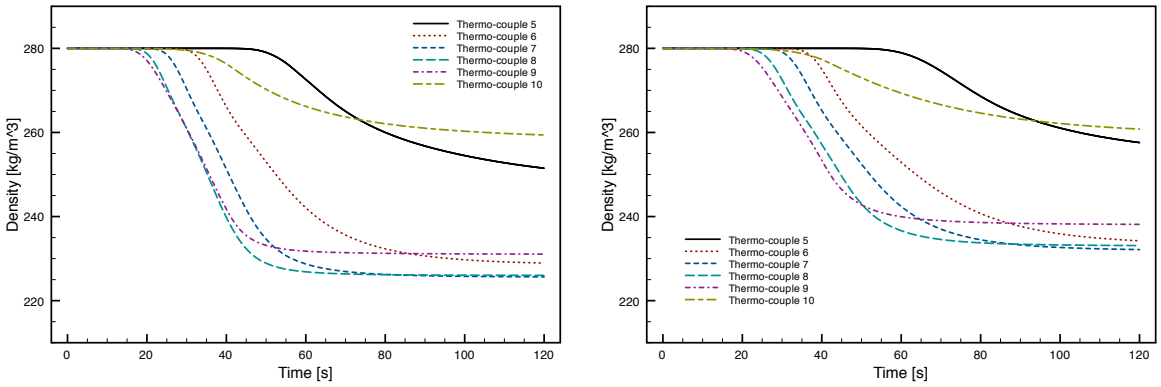

(a) Test 3.3

(b) Test 3.2

Figure 31. Density evolution of the thermo-couples 5 till 10.

DEVELOPMENT AND QUALIFICATION OF A LIGHT-WEIGHT ABLATOR AEROSHELL BREAD BOARD MODEL FOR MARTIAN MISSIONS

Kazuhisa Fujita, Toshiyuki Suzuki, Takuya Aoki, Toshio Ogasawara,

Yuichi Ishida, Hisako Gushima, and Naomi Takizawa
Japan Aerospace Exploration Agency
Fujita.kazuhisa@jaxa.jp

A bread board model (BBM) of the light-weight aeroshell consisting of the carbon-polyimide light-weight ablator and the CFRP honeycomb structure has been developed and qualified. In the early phase of BBM development, a large number of combinations of polyimide matrix, carbon fiber foam, and adhesive material were tested for screening through arc-heating tests as well as strength tests, and the best combination for the Martian atmospheric entry mission under consideration in Japan Aerospace Exploration Agency was finally selected. A BBM of 500 mm in diameter was designed and fabricated to examine validity of the process of manufacture and to estimate the fabrication cost for a flight model. The fabricated BBM, shown in Fig.1, was finally qualified through random/sinusoidal vibration tests, pyro shock tests, and thermal vacuum tests.

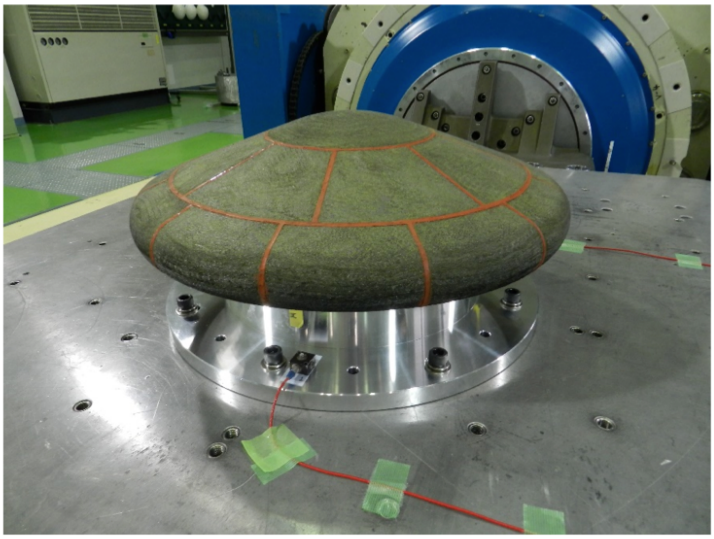

Figure 1: A bread board model of the light-weight aeroshell equipped with the carbon-polyimide light-weight ablator (mounted on the vibration test facility).

A LIGHT-WEIGHT ABLATIVE MATERIAL FOR RESEARCH PURPOSES

Ch. Zuber, Th. Rothermel, L.M.G.F.M. Walpot

German Aerospace Center
Linder Höhe, 51147 Cologne, Germany
thomas.rothermel@dlr.de

For the atmospheric re-entry of spacecraft from high energetic trajectories a high-performance thermal protection system (TPS) is necessary to withstand extreme heat fluxes. During sample return missions as well as the entry maneuver into the atmosphere of a gas giant like Jupiter thermal loads may exceed the loads of a re-entry maneuver from earth orbit by two or three orders of magnitude. Such missions are also extremely mass sensitive. At the Institute of Structures and Design of the German Aerospace Center such an ablative material is currently under development. The development started with extensive material screening tests with the intention to select the most promising resin, reinforcement fibre and structural concept combination for the light- weight TPS material In a second phase we looked into the details of manufacturing techniques for light-weight thermal protection materials. Based on our experience from the first phase we tried to develop a foam-like, microporous resin matrix structure, which combines high isolating properties with a closed-cell microstructure. We also consider a closed-cell microstructure to be important to avoid the penetration of hot gases into the material. The result of the work is a material called "ZURAM R", which survived a test in the plasma wind tunnel PWK1 (Institute of Space Systems, University of Stuttgart) at 12 MW/m^2 for 15 seconds with a moderate recession of averaged 1.8 mm (Figure 1) Considering the fact t hat for the use in an application today also good prediction of behavior and capabilities is necessary, recently a lot of effort is put into the development of state of the art tools (e.g. PATO [1], TACOT [2], Test Case Definition of the European Ablation Working Group [3] among others). One problem associated with testing the resulting numerical codes is the lack of a freely available ablative material as almost all of these materials are under some kind of restriction. Thus the material data used is either tied to literature data [3] or artificial material models [2]. Having a PICA (or ASTERM) -like material at hand that is noncommercial and not restricted, we therefore would like to invite interested parties to characterize the material, ZURAM R, to generate an open database for the participants to supplement respectively substitute material models like the TACOT [2] model by a real world material, which would allow the verification of the simulation of ablative processes. As a second element we would like to propose tests of the material in different plasma wind tunnel facilities under specific test conditions with the intention to gain knowledge about the comparability of tests conducted in facilities based upon different principles of operation, preferably at a common test condition (if exists).

Figure 1: Sample of ZURAM R after 15 sec at 12 MW/m^2 at PWK1 (IRS, University of Stuttgart)

1. REFERENCES

[1] Lachaud, J R; Mansour, N N: A pyrolysis and ablation toolbox based on OpenFOAM with application to material response under high enthalpy environments. *5th OpenFOAM Workshop*, Chalmers, Gothenburg, Sweden, June 21-24. 2010

[2] Lachaud, J R; Martin, A; van Eekelen, T; Cozmuta, I: Ablation test-case series #2: Numerical Simulation of Ablative-

Material Response - Version 2.8 - Feb. 6, 2012. *5th Ablation Workshop*, Lexington, Kentucky, February 28-March 1. 2012

[3] Reynier, Ph; Chambre, G: Test Case Definition of the European Ablation Working Group. Report. Contract 067/2007, ISA TN-04-2007. Ingnierie et Systmes Avancs. 2007-10

IN-SITU RECESSION MEASUREMENTS BY PHOTOGRAMMETRIC ABLATOR SURFACE ANALYSIS

Stefan Loehle

Universität Stuttgart, Institut für Raumfahrtsysteme
Stuttgart, Germany
loehle@irs.uni-stuttgart.de

Thomas Reimer

German Aerospace Center
Stuttgart, Germany

Alessandro Cefalu

Universität Stuttgart, Institut für Raumfahrtsysteme
Stuttgart, Germany

Extended Abstract

Experimental investigation of the thermochemical performance of heat shield materials is usually conducted in so–called plasma wind tunnels. The state of the art diagnostic tools are focusing on the measurement of surface temperatures, in-depth temperatures using thermocouples and spectroscopic diagnostics in order to investigate the plasma layer in front of the tested materials [1, 2]. Except for some specific procedures, i.e. laser recession measurements, an assessment of the surface geometry changes during testing is missing. The common approach to determine the material recession is to compare the sample thickness before and after the test, however, this method does not give insight into the transient processes.

These transient processes are important, in particular for modern lightweight ablators, and the ground testing methodology needs to be improved to enable a better understanding of these processes to be gained. The first attempts of measurements showed the principle feasibility of a modern data approach which was verified under lab conditions at room temperature with the focus on the equipment used and the types of materials to be tested [3].

In ground testing environments, surface recession and surface changes can be observed using optical methods. Very simple approaches are based on the observation of laser spots on the surface which change position when the material recesses [4]. This technology is also investigated by the authors in the plasma wind tunnels at IRS.

The approach presented in this paper follows the photogrammetric image analysis route. A combination of open source software tools and commercial programs have been used to analyse simultaneously acquired photographs of the recessing surface. Modern photogrammetric software tools are based on a pixelwise analysis allowing a high geometrical resolution and a comparably high accuracy. Two digital single lens reflex (DSLR) cameras were adapted for plasma wind tunnel purposes using fixed focal length (100mm) lenses.

Within the present study, first experimental results are presented from in–situ surface analysis of material probes surfaces using photogrammetric approaches.

The material tests within this study have been conducted in the plasma wind tunnel named PWK1. The probe is mounted on a moving platform inside the vacuum chamber (6 m in length and 2 m in diameter) which is connected to the in-house vacuum pumping system. The high enthalpy plasma generator RD5, a magnetoplasmadynamic arcjet [5], is mounted in the front lid of the vessel. Electric power is provided by a current-regulated thyristor rectifier consisting of six identical units supplying 1 MW each. Samples and measurement equipment is mounted in corresponding water-cooled probes. The probes are moved horizontally inside the chamber to adjust the heat load and total pressure. To increase the number of measurements possible during each experiment, some probes have been manufactured with two heads and so two tests can be performed within one experiment by rotating the probe. The present investigation has been conducted with a probe that is usually used for material investigation of ablative test materials [6, 7]. The probe material is a carbon preform of type CALCARB with a probe diameter of 40 mm. This material seems suitable for basic ablation testing and is also in use in other facilties [8].

A flow condition has been chosen which was investigated for ground tests to analye the Hayabusa re-entry in 2010 [9].

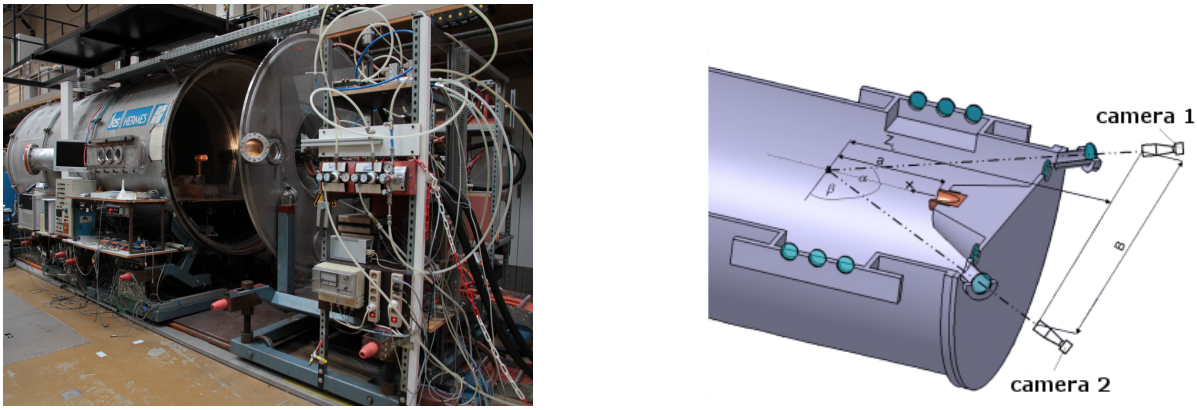

Figure 1: Plasma windtunnel PWK1 (left) and geoemtrical setup for the photogrammetry (right).

Fig 1 shows a photograph and a schematic of the setup using two cameras.

The images are acquired using two Canon EOS 60D digital single lens reflex (DSLR) cameras. The cameras are triggered simultaneously, within < 100 ms of each other, using a radio controlled trigger. For the present analysis a frame rate of one image per second (1 fps) has been realized. par Fig. 2 shows an image of the probe in the hot plasma flow.

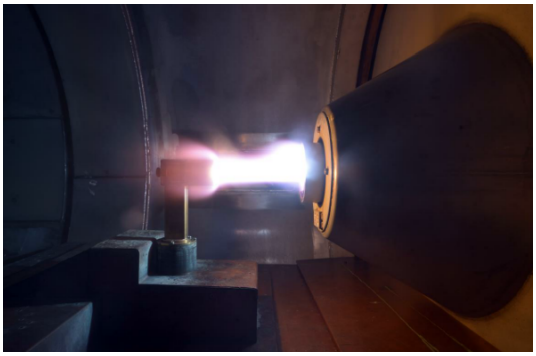

Figure 2: Probe during experiment.

During an experiment, the left and right cameras simultaneously acquire images. As an example, Fig. 3 shows the photographs taken at one instant in time.

The images shown here are slightly unfocussed which was the result of setting the manual focus prior to the test in low light conditions. However, the data is usable for photogrammetric evaluation. In the middle of the glowing sample, a little brighter spot is seen which a bore used for spectroscopic measurements that are ongoing in parallel [10, 11].

During this test, 9 image pairs have been acquired and analysed. The point cloud is plotted in Fig. 4. The colour scale is the recession in meters from the beginning of the test (0s) to the time of acquisition. So, the last image (14 s) shows the recession after 14 s.

The presentation will show the background theory and further evaluation of the data sets acquired in the plasma wind tunnel. A comparison to other diagnostic tools will be assessed.

1. REFERENCES

[1] Chen, Y.-K. and Milos, F. S., "Ablation and Thermal Response Program for Spacecraft Heatshield Analysis," *Journal of Spacecrafts and Rockets*, Vol. 36, No. 3, 1999.

[2] Löhle, S., Eichhorn, C., Steinbeck, A., Lein, S., Herdrich, G., Röser, H.-P., and Auweter-Kurtz, M., "Oxygen Plasma Flow Properties deduced from Laser-induced Fluorescence and Probe Measurements," *Applied Optics*, Vol. 47, No. 13, 2008, pp. 1837–1845.

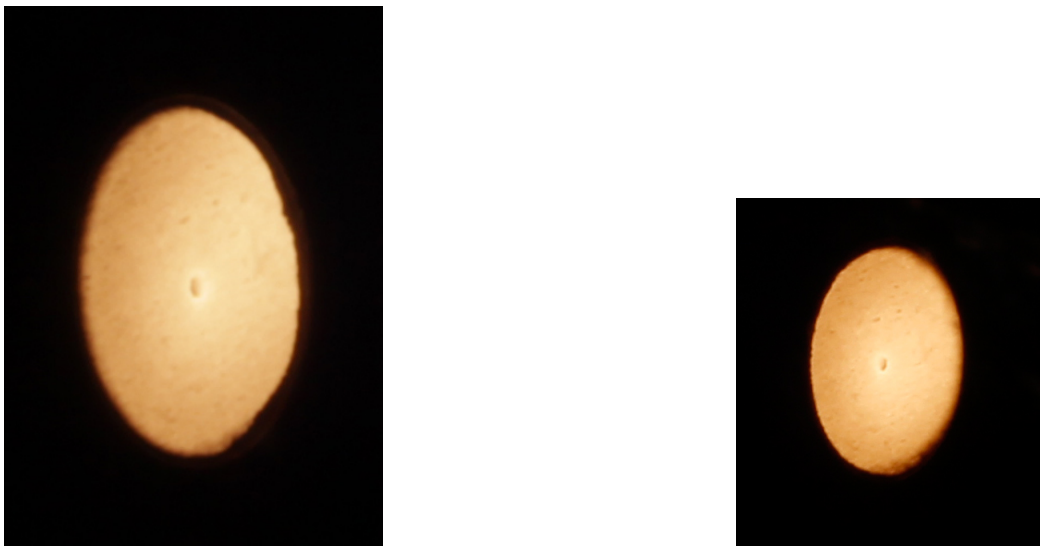

Figure 3: An example pair of images (left and right camera becomes left and right image) taken during the tests.

[3] Löhle, S. and Reimer, T., "Experimental Investigation of Photogrammetric Surface Analysis of Heat Shield Materials during Plasma Wind Tunnel Testing," *7th ESA Thermal Protection Workshop*, ESA, 2013.

[4] Sherrouse, P. and Carver, D., "Demonstrated Real-Time Recession Measurements of Flat Materials During Testing in High-Enthalpy Flows," *30th Aerospace Science Meeting and Exhibit*, AIAA, 1992.

[5] Auweter-Kurtz, M. and Wegmann, T., "Overview of IRS Plasma Wind Tunnel Facilities," *RTO AVT/VKI Special Course on Measurement Techniques for High Enthalpy Plasma Flows*, No. AC/323(AVT)TP/23 in RTO-EN-8, 2000.

[6] Eswein, N., Herdrich, G., Fasoulas, S., and Röser, H.-P., "Investigation of Graphite Ablation at IRS," *42nd Thermophysics Conference*, AIAA, 2011.

[7] Wernitz, R., Eichhorn, C., Herdrich, G., Löhle, S., Fasoulas, S., and Röser, H.-P., "Plasma Wind Tunnel Investigation of European Ablators in Air Using Emission Spectroscopy," *42nd AIAA Thermophysics Conference*, 2011.

[8] Helber, B., Chazot, O., Magin, T., and Hubin, A., "Ablation of carbon preform in the VKI Plasmatron," *43d Thermophysics Conference*, No. AIAA 2012-2876, AIAA, 2012.

[9] Löhle, S., Brandis, A., Hermann, T., and Peter, J., "Numerical Investigation of the Re-entry Flight of Hayabusa and Comparison to Flight and Ground Testing Data," *43rd AIAA Thermophysics Conference*, AIAA, LA, 2012.

[10] Hermann, T., Zander, F., Fulge, H., Löhle, S., and Fasoulas, S., "Experimental Setup for Vacuum Ultraviolet Spectroscopy for Earth Re-entry Testing," *30th Aerodynamic Measurement Technology and Ground Testing Conference*, AIAA, 2014, submitted.

[11] Löhle, S., Hermann, T., Zander, F., Fulge, H., and Marynowski, T., "Ablation Radiation Coupling Investigation in Earth Re-entry Using Plasma Wind Tunnel Experiments," *30th Aerodynamic Measurement Technology and Ground Testing Conference*, AIAA, 2014, submitted.

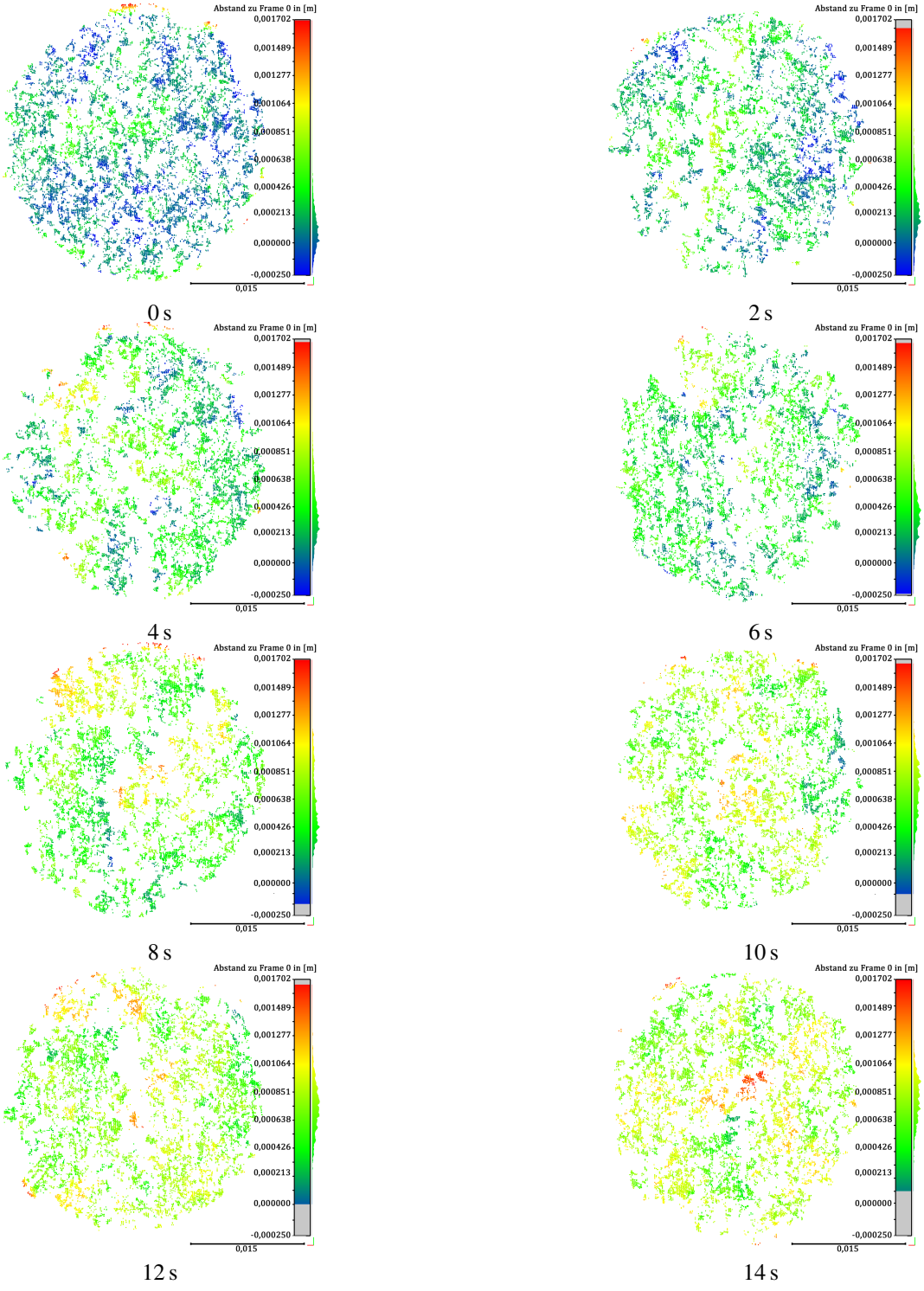

Figure 4: Photogrammetric result of Calcarb ablation during high enthalpy testing.

TOUGHCERAMR® HIGH TEMPERATURE STRUCTURAL & ABLATION COMPOSITE

Max SARDOU and Patricia SARDOU
Department of Mechanical Engineering
max.sardou@sardou.net

SARDOU SA, a French Research, Development, Design & Innovation Company created in 1980, has developed highly stressed composites since 33 years.

For intense, three dimensional shear loading fatigue. SARDOU SA have had to concentrate research on epoxy matrix in order to improve their life expectancy.

- This work has leaded us to develop a unique matrix which is a compound of organic epoxy and "mineral micro-reinforcing fasteners epoxy" called EPOSIL. Thanks to EPOSIL® it is now possible to produce damage tolerant structures and to improve by ten times their life expectancy.
- This concept has lead us to develop a though matrix for high temperature applications. this matrix is a compound of ceramic matrix and "mineral micro reinforcing fasteners" called TOUGHCERAM®

TPS and Rocket Nozzle (TPS-RN) STATE OF THE ART ANALYSIS

A lot of high temperature applications like TPS and Rockets Nozzle use:

- Carbon phenolic impregnated structure
- Ply by ply stratification

- Each layer is only glued to the next one by the matrix; so we get a very poor quality structure especially when we are close to matrix TG. Structure is then easy to delaminate. (FIG 1)
- In a TPS-RN application, in a few TENTH OF A SECOND temperature reach about 2500 to 3000°C inducing HIGH THERMAL STRESS.

Drawback of state of the art CARBON PHENOLIC structures:

-Is its poor Onset Temperature (as shown in the ATG measurement FIG 2) due to its organic resin we get high thermal dilatation , high thermal stress and easy delamination.

-There are a lot of questions about the future REACH & availability of PHENOLIC RESINS composites for TPS-RN applications

-In addition there are the same questions about the PHENOLIC RESINS used as a precursor in order to produce SiC TPS-RN by infusion.

A. TOUGHCERAM® FAMILY

Benefit of TOUGHCERAM® are:

- Their high Onset Temperature (FIG 3)
- Their interlocked strengthening micro staples (5 & 6)

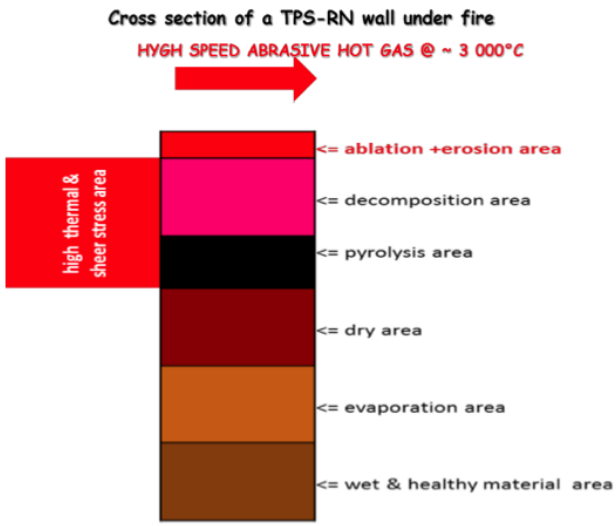

Figure 1: CROSS SECTION OF A "TPS-RN" UNDER FIRE

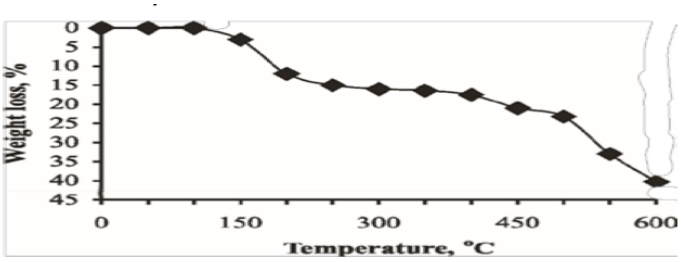

Figure 2: ATG OF CARBON PHENOLIC RESIN

- Their REACH COMPLIANCE
- Their low cost
- Their low density =1.5 (FIG 4)
- Their low thermal dilatation due to their ceramic resin.
- Their ease of production (exactly like a thermoset organic composite FIG 7, 8, 9) at 1263 °C a mulitisation reinforcing process occur.

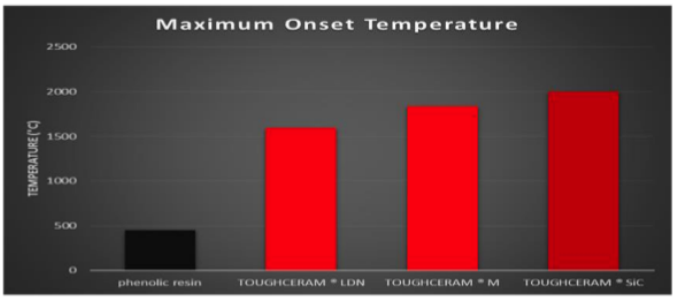

Figure 3: ONSET TEMPERATURE of TOUGHCERAM® FAMILY compared to CARBON PHENOLIC RESIN

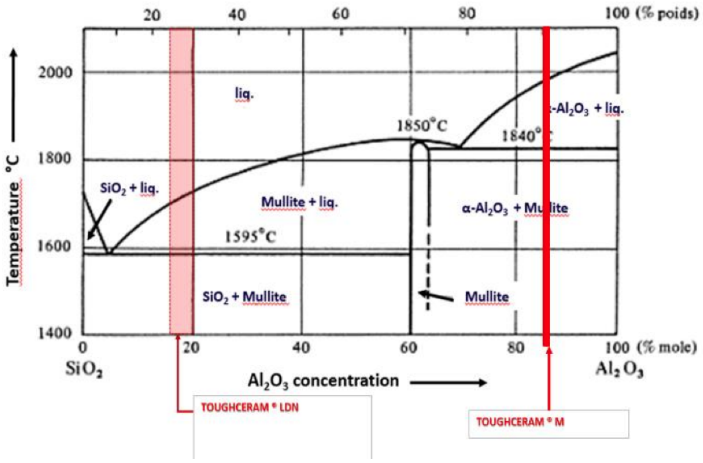

Figure 4: TOUGHCERAM® LDN& M

CONCLUSION: TOUGHCERAM® M

TOUGHCERAM® M is a compound of ultra-low cost, easy to use alkali resin comprising aluminum hydrate & metakaolin.

This system polymerize at only 60 °C!

Pyrogenic Dendritic Alumina, with high specific surface area, is added to the resin prior polymerization.

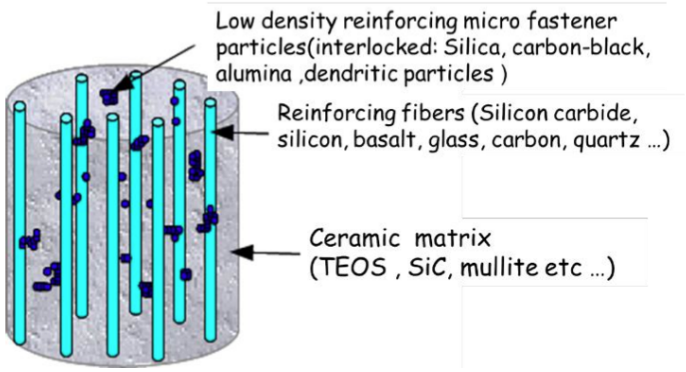

Figure 5: TOUGHCERAM® KEY STRUCTURE

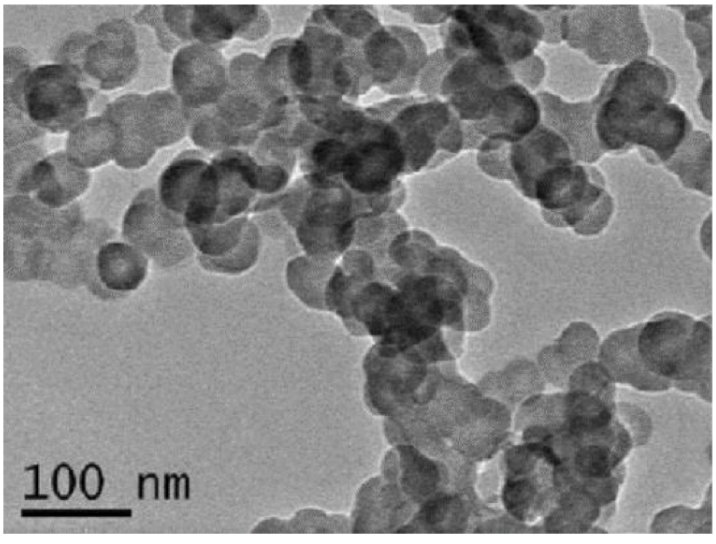

Figure 6: TOUGHCERAM® strengthening MICRO STAPLES

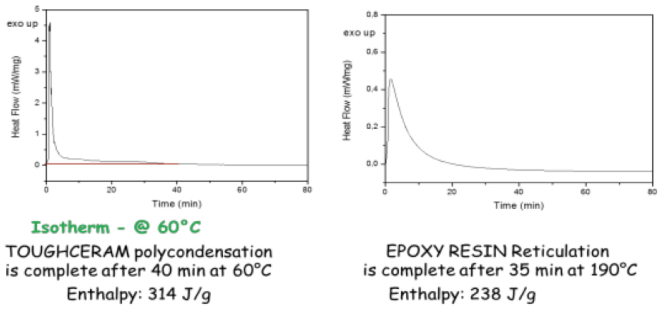

Figure 7: TOUGHCERAM® versus EPOXY POLYMERISATION

Figure 8: TOUGHCERAM® M processing steps

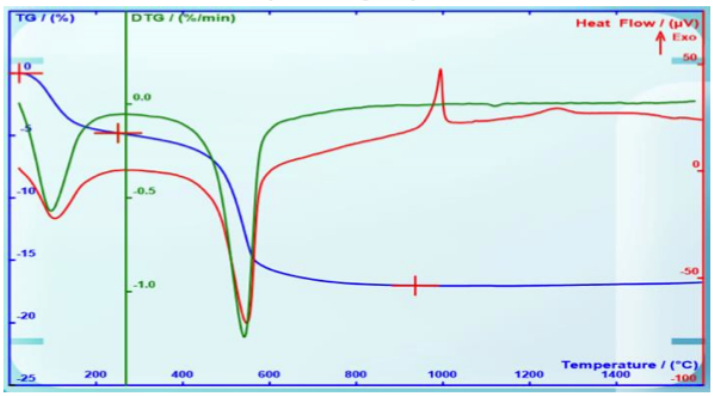

Figure 9: TOUGHCERAM® mulitisation at 1263 °C (ATG & DSC)

Sintering occur over 1263C under vacuum. During sintering aluminum, and silicon turn to a dense and INTERLOCKED MULITE needles NETWORK .20% POROUS. This NETWORK is an excellent thermal insulating & tough structure. Dendritic alumina micro staples network create an additional rigid light and tough interlocked microreinforcing continuum in the mulite matrix. Carbon or SiC structural fibers are imbedded in the composite (FIF 5). Mulite melt at 2000C and boil at 3000 °C. This set of temperatures is just perfect for ablative regime!

TOUGHCERAM ® SiC

TOUGHCERAM® SiC PROCESSING

We use EPOCARB® which is a compound of low cost, easy to use organic epoxy and carbon black epoxy. Carbon black is highly dendritic and has a high specific surface area. During the pyrolysis epoxy leave graphite binder, connecting a dense carbon black interlocked network. Liquid SILICON Infiltration at 1410 °C (LSI) is done under vacuum. During LSI graphite, and carbon black network turn to a dense and POROUS SiC NETWORK. This solution is an excellent thermal insulating & tough structure. EPOCARB® compound offer low pollution, is REACH compliant and easy to use.

EPOCARB® is made with a DGEBA organic epoxy, compounded with a high content of "carbon black epoxy". During pyrolysis graphite, due to degradation of the DGEBA, interconnect dendritic carbon black micro staples creating a compact interlocked network. During the silicon infusion, graphite convert to SiC ceramic matrix and carbon black network create a rigid light and tough interlocked microreinforcing staples continuum. (FIG10). Carbon or SiC structural fibers are imbedded in the composite (FIF 5). SiC sublimation occur at 2700 °C this sublimation property is just perfect for ablative regime!

B. INTERLOCKED 3D FIBERS

We propose a short distance interlocked 3D fibber preform in order to resist to delamination due to thermal chocks and dilatation, this is better than state of the art 2D or stitched solution.

Benefit of interlocked 3D structure are:

1) as each layer is attached by reinforcing fibers to the next one, we get a very strong reinforcing structure impossible to delaminate.

2) as interlocking fibbers goes only from one layer to the next one, it is a failsafe design, even if interlocking fibers are cut on the surface of the composite there is no dramatic delamination.

3) as interlocking fibbers goes only from one layer to the next one, this limit the thermal conduction inward the material.

REMOTE RECESSION SENSING OF ABLATIVE HEAT SHIELD MATERIALS

Michael W. Winter

Department of Mechanical Engineering
University of Kentucky, Lexington, KY
Michael.Winter@uky.edu

Margaret Stackpoole

NASA Ames Research Center, Moffett Field, CA

Anuscheh Nawaz

Sierra Lobo, Inc.
NASA Ames Research Center, Moffett Field, CA

Gregory Lewis Gonzales

ERC, Inc.
NASA Ames Research Center, Moffett Field, CA

Thanh Ho
Universities Space Research Association (USRA)
NASA Ames Research Center

Tests were performed to demonstrate the feasibility of a new method of measuring surface recession of a material sample during arc-jet testing in the NASA Ames mArc subscale developmental facility. The measurement principle was inspired through tracer elements such as Ca and Na which were seen in the spectra taken during the airborne observation campaign of the Stardust re-entry and which could be clearly observed standing out against the emission spectra emitted by post shock layer and glowing surface of the re-entry capsule. The measurement principle involves seeding of the heat shield materials at a defined depth with tracer elements which show strong and characteristic emission lines in the post shock plasma. Once the material recession reaches the seeding depth, these elements get into the hot plasma and show up in the emission spectra. The methodology was successfully demonstrated during arc-jet testing of phenolic impregnated carbon ablator (PICA) material which was seeded in depth with a mixture of NaCl and MgCl in powder form. In the emission spectroscopy data, the emission lines of Mg and Na showed up about 1.5s after probe insertion into the arc-jet plasma and vanished after another 2.5 seconds when recession had consumed the seeding material. From these data, a recession rate of about 1 mm/s is estimated. The heat flux during the test was measured to be 2575 W/cm^2 on a hemispherical heat flux probe which corresponds to a heat flux of 1036 W/cm^2 on the rectangular test articles. An estimate for a lower limit of the surface temperature of 2800K during the test was obtained by fitting Planck radiation to the continuum spectra emitted by the PICA sample. Typical recession rates of PICA during testing in the large arc-jet facilities at similar test conditions are reported to be on the order of 0.05 to 0.1cm/sec which agrees well with the recession rates of 0.05-0.06 cm/s estimated from the emission spectroscopy data. Further tests under better controlled conditions are suggested to quantify this measurement method. Through a different choice of seeding materials with lower melting point, an extension of the measurement principle to monitor char depth seems feasible but was not yet demonstrated. Possible applications besides ground testing are recession and possibly char depth measurements during real re-entry. Detection through emission spectroscopy could be accomplished through ground based or airborne observation as performed during the Stardust and Hayabusa re-entries, or through on-board spectrometers. A suitable mission would be the re-entry of the OSIRIS-REX mission planned for late 2023. The measured data are presented and interpreted, the results and details of future applications are discussed.

MEASUREMENTS OF ABLATION SPECIES IN AN AIR PLASMA/ASTERM ABLATING BOUNDARY LAYER

Megan MacDonald, Pierre Mariotto, Christophe Laux

Laboratoire EM2C
Ecole Centrale Paris, France
megan.mac-donald@ecp.fr

Fabian Zander

Institut für Rahmfahrtsysteme
Stuttgart, Germany

Ablative materials have long been employed to protect spacecraft from the extreme environment of atmospheric entry. Current studies strive to increase the efficiency of such materials and understand the physics behind the various mechanisms of ablation. Measurements of the species concentrations, plasma and material temperatures, and heat fluxes in ground test facilities lead to a better understanding of these physical processes and therefore more accurate modeling and design capabilities.

To this end, experiments were performed in an air plasma produced by a 50 kW inductively coupled plasma torch. Measurements of key species profiles through the boundary layer, the plasma temperature profile, and the surface temperature are reported.

The facility and diagnostic setup has been described in detail in Ref. [MacDonald 2014 JTHT] and a general schematic is shown in Fig. 1.

The current setup differs from that described earlier only in that the plasma power has been increased to 8 kW, the 2 cm exit nozzle of the torch has been used for the current study, and the material sample diameter has been decreased to 1.5 cm. These modifications increase the heat flux delivered to the sample to approximately 5 MW/m^2.

The material studied here is ASTERM, a carbon fiber matrix injected with a phenolic resin that has recently been developed by EADS Astrium ST as a new European low- density phenolic ablator.

The plasma temperature for this torch configuration is approximately 3000 K. Material surface temperature reached approximately 2800 K as measured by a fit to the gray body curve from spectral measurements of the material surface. The Two Color Ratio Pyrometry (TCRP) method was also employed for surface temperature measurements; an example of an unprocessed image is shown in Fig. 2.

Calibrated intensity profiles through the boundary layer have been measured for the following species: C2, CH, NH, O, N, N2, CN, Na, Ca, and Ba. An extract of the spectral data obtained is shown in Fig. 3.

References

1. MacDonald, M.E., Jacobs, C.M., Laux, C.O., Zander, F., Morgan, R.G., "*Measurements of Air Plasma/Ablator Interactions in an Inductively Coupled Plasma Torch*, submitted to Journal of Thermophysics and Heat Transfer, February 2014.

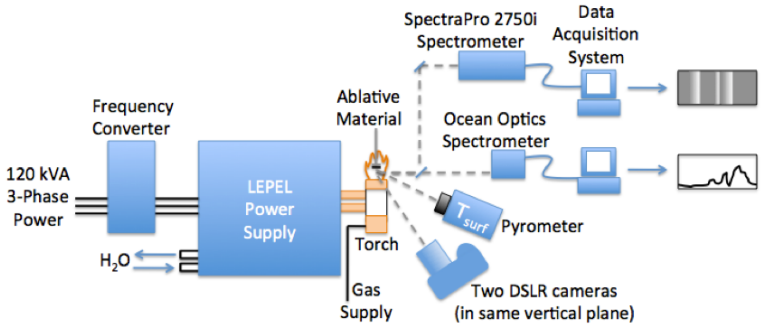

Figure 1: Facility and diagnostics overview

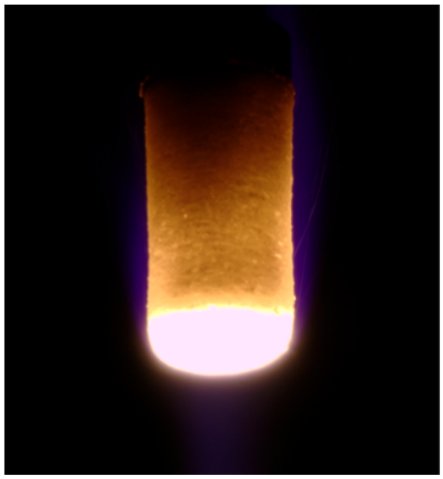

Figure 2: Unprocessed TCRP image of ASTERM ablation

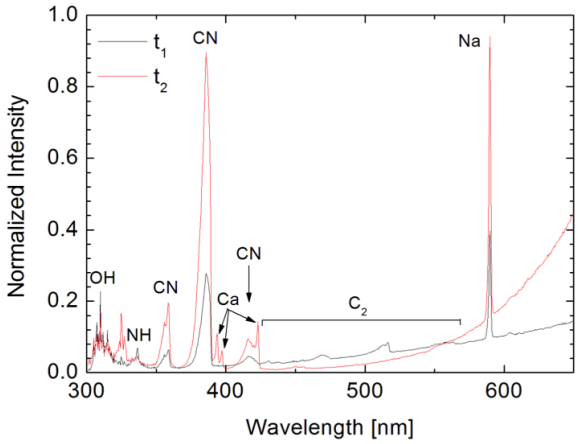

Figure 3: Evidence of OH, NH, CN, Ca, C2, and Na in the boundary layer of ablating ASTERM

EXPERIMENTAL DETERMINATION OF PYROLYSIS PRODUCTS FROM CARBON/RESIN ABLATIVE MATERIALS

Hsi-Wu Wong and Jay Peck

Aerodyne Research Inc.
Billerica, Massachusetts
hwwong@aerodyne.com

Guillaume Reinisch

Institute for Computational Engineering and Sciences
University of Texas at Austin, Austin, Texas
guillaume@ices.utexas.edu

Jean Lachaud

University of California, Santa Cruz
Moffett Field, California
jlachaud@ucsc.edu

Nagi N. Mansour

NASA Ames Research Center
Moffett Field, California
nagi.n.mansour@nasa.gov

Batch pyrolysis experiments of a generic phenolic resin and a carbon/resin ablative material were performed using a step-wise heating procedure in a 50 K increment from room temperature up to 1250 K. The samples were loaded in a reactor assembly specially designed and built for this study. The mass loss was measured after each 50 K step. Detailed yields of water vapor, permanent gases (hydrogen, methane, carbon monoxide, and carbon dioxide), light hydrocarbons (C2 to C4 hydrocarbons), aromatic products (benzene, toluene, and xylene), and aromatic alcohols (phenol, cresol, methylphenol, and dimethylphenol) were determined using gas-chromatography (GC) techniques. Reaction pressure of each step was also measured in real-time. Mass loss, reaction pressure, and product yields as a function of reaction temperature will be presented in this talk.

CHARACTERIZATION OF THE FLOW FIELD OVER AN ABLATIVE SURFACE

Michael Allard and Christopher White

Department of Mechanical Engineering
University of New Hampshire, Durham, NH
Michael.Allard@wildcats.unh.edu

Yves Dubief

Department of Mechanical Engineering
University of Vermont, Burlington, VT
ydubief@uvm.edu

Ablation experiments are performed in a small-scale wind tunnel to investigate the response of turbulence to wall recession and emergence of roughness (ablation patterns). The flow being investigated is a spatially developing heated boundary layer over a wall made of paraffin wax, chosen based on its low melt point temperature. Several variations of the inlet conditions, both for flow and temperature, are used to study the temporal and spatial development of ablation driven by coherent structures, such as vortices. Characterization and comparison of velocity and thermal fields, using particle image velocimetry and thermocouples respectively, over ablative and non-ablative surfaces are reported in addition to qualitative observations of ablation patterns. This work is part of a collaborative effort between numerical simulations and experiments to investigate the fundamental coupling mechanisms between an ablative wall and turbulence.

List of Authors